

# Sound localization using an array of Acoustic Vector Sensors

Mainstation data processing

Hans Okkerman (4290453) and Youri Westhoek (4281780)  
Version: 2.0

Bachelor Graduation Project

# **Sound localization using an array of Acoustic Vector Sensors**

## **Mainstation data processing**

BACHELOR GRADUATION PROJECT

Hans Okkerman (4290453) and Youri Westhoek (4281780)

July 10, 2017

Faculty of Electrical Engineering, Mathematics and Computer Science (EEMCS)  
Delft University of Technology

## **ABSTRACT**

In this thesis five different Direction Of Arrival algorithms will be developed for use with Microflown's Acoustic Vector Sensors, which will determine the direction an acoustic signal originates from. These algorithms will run on a main-station that will remotely receive data from an array of Acoustic Vector Sensors. The performance of these algorithms is examined using simulations and measurements obtained by a test setup. Finally, it is discussed under what circumstances which algorithm delivers the best performance.



---

# Contents

<b>1</b>	<b>Introduction</b>	<b>1</b>
1-1	Background . . . . .	1
1-2	System overview . . . . .	2
1-3	Problem . . . . .	3
1-4	Synopsis . . . . .	4
1-5	Requirements . . . . .	6
<b>2</b>	<b>Datamodels</b>	<b>7</b>
2-1	Data model of a single AVS . . . . .	7
2-2	Data model of an array of AVSs . . . . .	8
<b>3</b>	<b>Single AVS based DOA estimation</b>	<b>11</b>
3-1	Time domain approach . . . . .	12
3-2	Frequency domain approach . . . . .	13
3-3	Simulation . . . . .	14
3-3-1	Simulation with an impulse signal . . . . .	14
3-3-2	Simulation with a sinusoidal signal . . . . .	15
3-4	Discussion . . . . .	18
<b>4</b>	<b>Linear phased array based DOA estimation</b>	<b>19</b>
4-1	Time Delay Of Arrival . . . . .	20
4-2	Beamforming . . . . .	22
4-3	Simulation . . . . .	26
4-3-1	TDOA . . . . .	26
4-3-2	Beamforming . . . . .	27
4-4	Discussion . . . . .	30

---

<b>5</b>	<b>Results</b>	<b>31</b>
5-1	Measurement setup . . . . .	32
5-2	Measurement results . . . . .	34
5-2-1	Intrinsic . . . . .	34
5-2-2	TDOA . . . . .	36
5-2-3	Beamforming . . . . .	37
<b>6</b>	<b>Discussion</b>	<b>41</b>
<b>7</b>	<b>Conclusion</b>	<b>43</b>

---

# Introduction

## 1-1 Background

Locating the source of a signal has long been a subject of interest. It plays a role in radar systems, sonar and even seismic research. Localization of acoustic signals can be useful to automatically direct a camera or microphone towards a speaker in a lecture hall [1], to detect the use of illegal fireworks or on the battlefield to passively detect the location of snipers without necessarily being able to see them [2].

Since pressure sensors are scalar and do not have intrinsic directivity, sound localization is usually done with multiple pressure sensors (microphones) placed in an array. The most explored way to determine the direction to an acoustic source is Time Delay Of Arrival (TDOA). This makes use of the delay between when an acoustic signal arrives at each sensor to determine the angle of arrival [3]. Another technique is beamforming. Beamforming instead works by optimizing the sum of the signals coming from all the sensors in an array to find the direction a signal of interest is coming from and to filter out signals that are not [4] [5]. There are several types of beamforming algorithms that perform this task. The ones that are explored in this thesis are Delay And Sum (DAS) [6] and Minimum Variance Distortionless Response (MVDR) [7] beamforming.

One problem these type of arrays have is that they become rather large if they have to localize low-frequency sources. To avoid spatial filtering the distance between the microphones needs to be at least half of the wavelength [8] of the sound to be localized. This means that for low frequency sources, the array length needs to be multiple meters.

At any point in space, a sound field can be completely described by sound pressure (scalar) and acoustic particle velocity (vector). Recently a new type of acoustic sensor became available; the AVS or Acoustic Vector Sensor. This sensor contains a standard pressure sensor as well as two or three orthogonal particle velocity sensors to perform 2D or 3D measurements respectively. These sensors make it possible to use a smaller array size while getting the same results [9]. The AVS used in this project is developed by Microflown Technologies and can be seen in Figure 1-1. As stated in [10], each of the particle velocity sensors consist of two extremely sensitive heated wires. When air flows across the wires, the first wire cools down a little and due to heat transfer the air picks up some heat. Because the heated air now cools down the second wire, this wire cools down less than the first wire.

Sound localization using an  
array of Acoustic Vector Sensors

This results in both wires having different temperatures, and therefore different resistances, causing a voltage difference proportional to the particle velocity. The result is also directional, since reversing the airflow will result in a reversed temperature difference. Combining three Microflow sensors gives you the ability to measure the x, y and z direction of incoming sound waves. This means that the AVS has intrinsic directive properties.

These orthogonal vector measurements make it possible to determine the location of an acoustic source with only one AVS, allowing for arrays with less elements and thus a smaller size. Furthermore, with a wide operational range ranging from 0.1Hz to 10kHz they can still provide directional information at low frequencies with small array sizes where regular pressure sensors cannot [11].

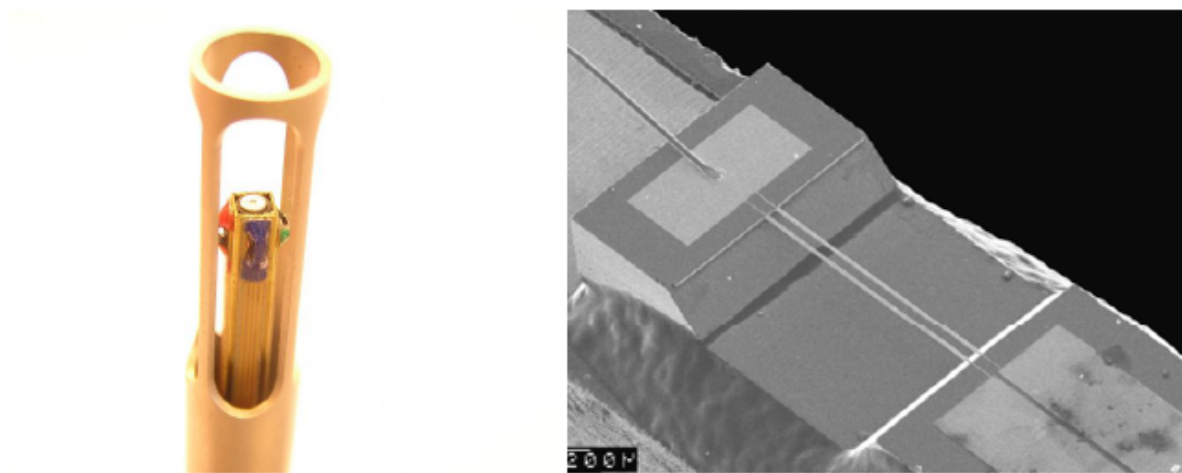


**Figure 1-1:** An Acoustic Vector Sensor and closeup of a particle velocity sensor [12] [10]

## 1-2 System overview

In Figure 1-2 the framework of the project is shown. At stage 1, the AVS array is shown. All of the sensors measure the sound pressure, as well as the x and y velocity of the sound wave.

In the second stage, the sensor data is processed by a DSP. Each AVS is connected to its own DSP. These are used to do on-site calculations to minimize the amount of data that has to be sent to the main station, while making sure that all the important information is transmitted. This is important because the bandwidth between the DSPs and the main station is limited.

The third stage is the main station. The main station receives the data sent from the DSPs and processes it. The main goal of this mainstation is to determine the direction a detected sound originated from. The main station is responsible for monitoring the status of the sensor network. This report will focus on the dataprocessing at the *Mainstation* and its possibilities to estimate the locations of sound sources.

Sound localization using an  
array of Acoustic Vector Sensors

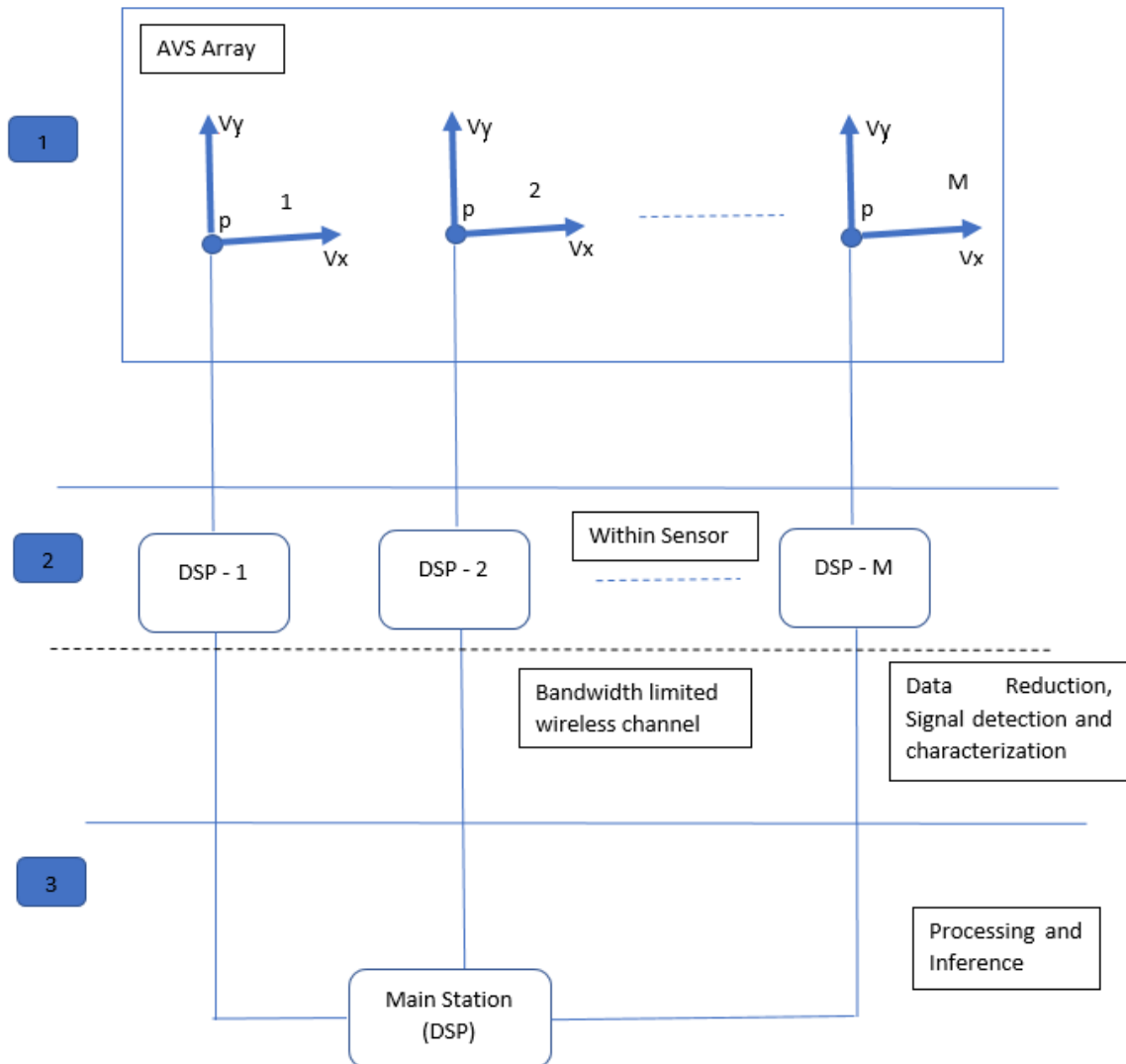


Figure 1-2: System overview

## 1-3 Problem

The Mainstation will not necessarily be close to the array. For example, there could be a stationary array for monitoring enemy territory and border control while the Mainstation is being operated on a (safe) remote location. Another possibility would be that the array is mounted to a military vehicle to give soldiers environmental awareness. As such the station may receive limited amounts of information. The goal of this project is to design a Mainstation that functions in such situations. This means that it must be able to locate multiple signal types, such as those from drones, explosions and gunshots. For this localization, far-field signals may be assumed.

Sound localization using an array of Acoustic Vector Sensors

The type of a signal influences the way its data has to be processed for source localisation. Based on the received data regarding signal type, the mainstation must choose the most accurate localization algorithm. This algorithm will run in Matlab with its resulting DOA estimation as output. Here it is assumed the DSP units of Figure 1-2 give as outputs: The measured data, the type of the signal: impulse or sinusoidal and in case of a sinusoidal signal the main frequency.

Also the signal to noise ratio's of the received signals have to be taken into account since for far-field situations the SNR can get quite low. The SNR at which the DSP can still detect a signal is  $-2dB$ , so Mainstation should be able to locate a sound signal received with this SNR.

Since Mainstation will have a wireless connection to the AVS array, one of the challenges is to minimize the data traffic from the DSP modules to Mainstation. As such Mainstation will most likely have to receive small data packets from each sensor and use those to determine the location of the source as seen from the array.

In this report an attempt will be made at solving these problems.

## 1-4 Synopsis

The rest of this thesis will be covered in the following order:

### **Chapter 2:**

In this chapter, the data models used in this thesis will be discussed. First the data model of the received signal for a single AVS is given. After that the datamodel of the received signal for an linear phased AVS array is given.

### **Chapter 3:**

This chapter shows the development of two DOA algorithms that make use of the intrinsic directional properties of the AVS. One that uses the time-domain, and one that works in the frequency-domain. Finally simulation results are discussed regarding the signal length and the signal to noise ratio.

### **Chapter 4:**

This chapter explains three linear phased array approaches for DOA estimation. These three approaches are: Time Delay of Arrival, Delay and Sum beamforming and Minimum Variance Distortionless Response beamforming. Finally simulation results are discussed regarding the signal length and the signal to noise ratio.

### **Chapter 5:**

In this chapter the performance of the discussed DOA approaches will be tested based on measurement-data taken from a real test setup.

### **Chapter 6:**

Here the results of the simulations and those of the real measurements will be compared. Any large

differences are discussed and recommendations for further development are mentioned.

**Chapter 7:**

Finally a conclusion will be drawn on which algorithm is best suited for which situation as well as how well the developed system complies with the system requirements.

## 1-5 Requirements

The following requirements are imposed on the system to be considered successful:

- Mainstation must be able to estimate the direction of arrival of a sound signal in 2D.
- The DOA of a signal must be detected within a 5 degree accuracy.
- Mainstation must be able to successfully find the DOA of an impulse and a sinusoidal wave.
- The DOA estimation have to be done with a minimal amount of signal data.
- The computational complexity must be low enough so that the DOA computation can keep up with the received data. I.e. the calculation must not take longer than the time it took to collect the data.
- DOA estimation needs to be possible from a signal to noise ratio of  $-2dB$  and up.

---

# Datamodels

In this chapter the data model of the signal received by a single acoustic vector sensor is explained. After that, this model will be expanded to one for an array of AVSs. Since one of the requirements is to localize a sound source in 2D space, the data model is depicted for source located in a  $\mathbb{R}^2$  scenario.

## 2-1 Data model of a single AVS

The measured data of an acoustic vector sensor consists of three streams: the pressure data  $P$ , the x component of the particle velocity data  $v_x$  and the y component of the particle velocity data  $v_y$ . The relation between the pressure and velocity data at a point in space is shown in Equation 2-1 [13]. Where  $\mathbf{u}$  is the unit vector pointing from the AVS towards the source,  $\rho$  is the density of the medium,  $c$  is the speed of sound in this medium and  $\rho \cdot c$  is the characteristic acoustic impedance of the medium.

$$v(t) = \frac{-\mathbf{u}}{\rho \cdot c} \cdot p(t) \quad (2-1)$$

Using the linear relationship  $\rho c$  of Equation 2-1 the pressure data  $P$  can be normalised to the same order of magnitude as the velocity data. Figure 2-1 then shows how the particle velocity components give directionality to the normalized pressure data received.

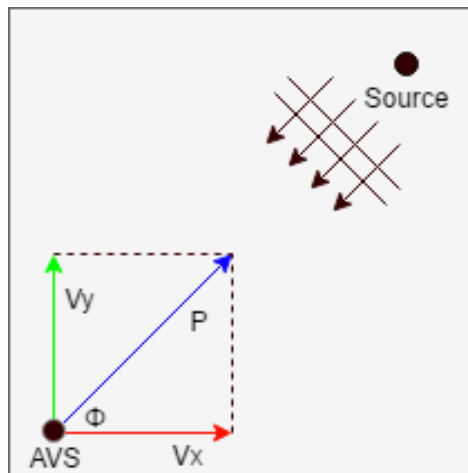


**Figure 2-1:** A visual representation of the directionality of an AVS

With this knowledge the signal received  $y(t)$  at an AVS can be represented as [14][15]:

$$y(t) = \begin{bmatrix} P \\ v_x \\ v_y \end{bmatrix} = \begin{bmatrix} \frac{1}{\rho c} \\ \cos \phi \\ \sin \phi \end{bmatrix} s(t) + n(t) \in \mathbb{C}^{3 \times 1} \quad (2-2)$$

Where  $s(t)$  is the signal coming from a source,  $n(t)$  is the noise present in the received signal and  $\phi$  is the angle of arrival from the source.

## 2-2 Data model of an array of AVSs

When modeling a linearly phased array of AVS's this model can be expanded. Now the source signal is received at multiple sensors which are linearly spaced across the x-axis, as shown in Figure 2-2. This means the time instant at which the sound wave is perceived will be different for each of the AVSs. To model this a phase delay vector  $D$  is created using the inter spacing  $d$  of the array and the spatial frequency of the source signal  $k = \frac{2\pi}{\lambda}$ . In Equation 2-3  $D$  is given for an array of  $M$  AVSs. Assumed in this report is that the first element of the array is located at the origin  $[0 \ 0]$ .

$$D = \begin{bmatrix} 1 & e^{i*k*d*\cos \phi} & \dots & e^{i*k*(M-1)*d*\cos \phi} \end{bmatrix}^T \in \mathbb{C}^{M \times 1} \quad (2-3)$$

The received signal at an array of AVSs then becomes:

$$y(t) = D \otimes \begin{bmatrix} \frac{1}{\rho c} \\ \cos \phi \\ \sin \phi \end{bmatrix} s(t) + n(t) \in \mathbb{C}^{3M \times 1} \quad (2-4)$$

Where  $\otimes$  denotes the Kronecker-product.

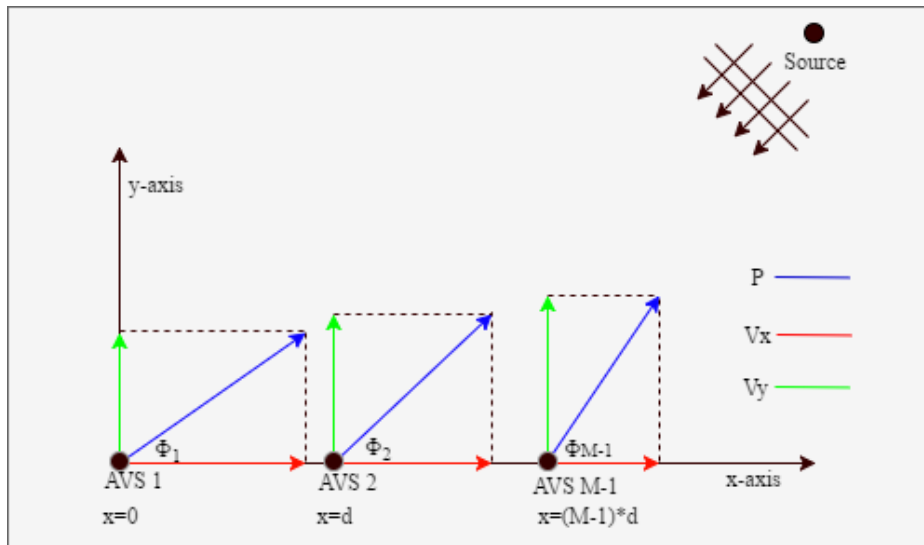


**Figure 2-2:** A near-field visual representation of an array of AVSs

For a far-field source the direction of arrival of the sound wave will be the same for every AVS in the array. However in near-field the DOA will be different for each AVS, like depicted in Figure 2-2. To compensate for a near-field scenario in the data model the angle per AVS has to be adjusted. This can be done using the geometry of the array and the distances  $[r_1 \ r_2 \ \dots \ r_M]$  where  $r_M$  corresponds to the distance from AVS number  $M$  to the source. Resulting in the data model in Equation 2-5 [16].

$$y(t) = \begin{bmatrix} 1 \cdot \begin{bmatrix} \frac{1}{\rho c} \\ \cos \phi_1 \\ \sin \phi_1 \end{bmatrix} \\ e^{i*k*(r_2-r_1)} \cdot \begin{bmatrix} \frac{1}{\rho c} \\ \cos \phi_2 \\ \sin \phi_2 \end{bmatrix} \\ \vdots \\ e^{i*k*(r_M-r_1)} \cdot \begin{bmatrix} \frac{1}{\rho c} \\ \cos \phi_M \\ \sin \phi_M \end{bmatrix} \end{bmatrix} s(t) + n(t) \in \mathbb{C}^{3M \times 1} \quad (2-5)$$

Usually the distance to a source is unknown, in that case a far-field source is assumed. This is a valid assumption regarding the expected use-cases of the system. For a far-field scenario, the angle can be held the same for every AVS in the array as in Equation 2-6.

$$y(t) = \begin{bmatrix} 1 \cdot \begin{bmatrix} \frac{1}{\rho c} \\ \cos \phi \\ \sin \phi \end{bmatrix} \\ e^{i*k*d*\cos(\phi)} \cdot \begin{bmatrix} \frac{1}{\rho c} \\ \cos \phi \\ \sin \phi \end{bmatrix} \\ \vdots \\ e^{i*k*(M-1)*d*\cos(\phi)} \cdot \begin{bmatrix} \frac{1}{\rho c} \\ \cos \phi \\ \sin \phi \end{bmatrix} \end{bmatrix} s(t) + n(t) \in \mathbb{C}^{3M \times 1} \quad (2-6)$$

This model can be reduced to Equation 2-7 for simplicity's sake.

$$y(t) = A(\phi)s(t) + n(t) \in \mathbb{C}^{3M \times 1} \quad (2-7)$$

Where  $A(\phi) = [a(\phi) \ a(\theta) \ \dots \ a(\gamma)]$ ; a collection of incoming signal DOA's corresponding to the signals present in  $s(t)$ . For a single source  $A(\phi) = a(\phi)$ .

Sound localization using an  
array of Acoustic Vector Sensors



---

# Single AVS based DOA estimation

The Acoustic Velocity Sensor has the unique possibility to estimate the Direction of Arrival of an incoming sound-wave on its own due to its directional properties. In this section a Time-domain and a Frequency-domain approach for using these intrinsic directional properties are developed. First the offered approaches are explained after which they are validated with simulation results.

### 3-1 Time domain approach

A possible way to give a DOA estimation is by directly looking at the (discrete) time domain particle velocity components of the received data stream;  $v_x$  and  $v_y$ . First the particle velocity components are multiplied element-wise with the respective pressure component of the received data stream. This will provide a clearer image of the direction, an example of which can be seen in Figure 3-1 for a signal originating at 150 degrees. If the signal arrives from the other side, i.e. 30 degrees, the resulting plot would be mostly positive instead as the pressure signal would remain the same while the vector signal is inverted. Now, an estimation of the angle of arrival can be made by taking the arctangens of the mean values of the results. This process is displayed in Equation 3-1.

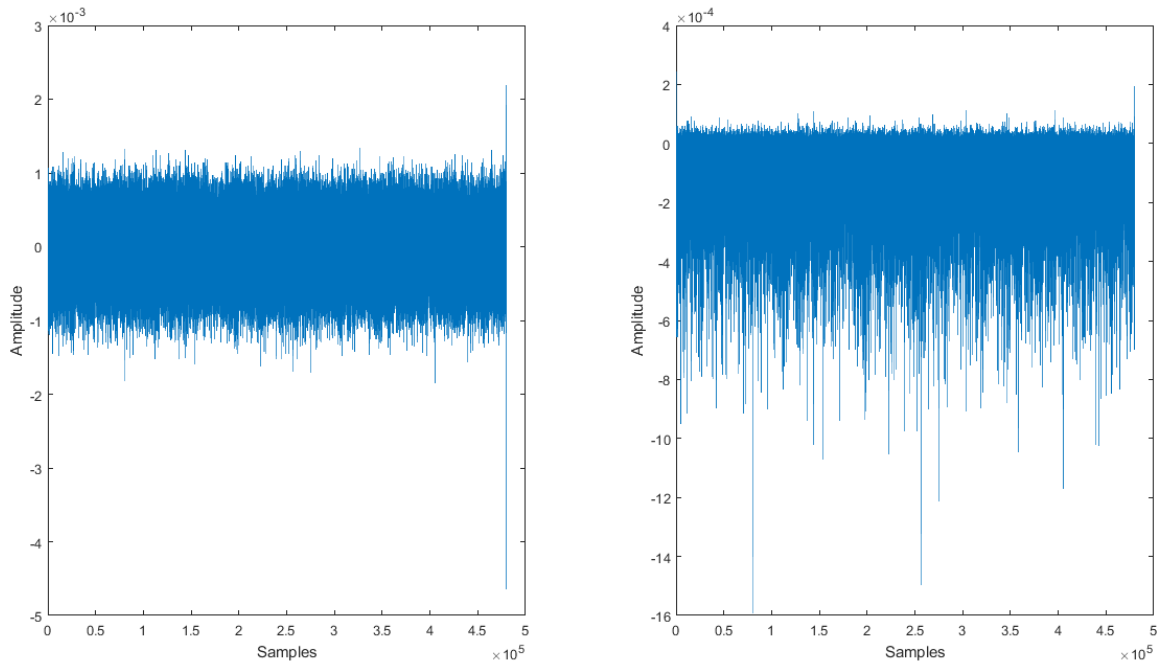


**Figure 3-1:** Received  $v_x$  signal of white noise with a DOA of 150 degrees and the same signal after multiplication with the pressure sensor data.

$$\phi_{DOA} = \arctan \left( \frac{\frac{1}{N} \sum_{n=1}^N v_y(n) \cdot p(n)}{\frac{1}{N} \sum_{n=1}^N v_x(n) \cdot p(n)} \right) \quad (3-1)$$

## 3-2 Frequency domain approach

By taking a look at the frequency spectrum of the received  $v_x$  and  $v_y$  a similar approach as the above offered time domain approach could be taken. A DOA estimation can be made by examining the spectra of  $v_x$  and  $v_y$ . When the characteristic frequency range of the signal is known, a frequency bin can be handled in which the amplitude of the spectra of the signals are analyzed. The accuracy of the signal detection unit is given to be  $\pm 20 Hz$ , so the frequency bin handled is  $\pm 20 Hz$  around the detected carrier-frequency.

First the Fast Fourier Transform (FFT) of both the particle velocity components of the received data is taken. Next a frequency bin is created around the given carrier of  $F_{carrier} - 20$  to  $F_{carrier} + 20 Hz$ . Now the direction of arrival is estimated as in Equation 3-2 by taking the arctangens of the maximum values of  $V_Y$  and  $V_X$  within this bin. An example of the resulting spectra can be found in Figure 3-2. The output for this example would be an estimated DOA of 33 degrees.

$$\phi_{estimation} = \arctan\left(\frac{V_{Ymax}}{V_{Xmax}}\right) \quad (3-2)$$

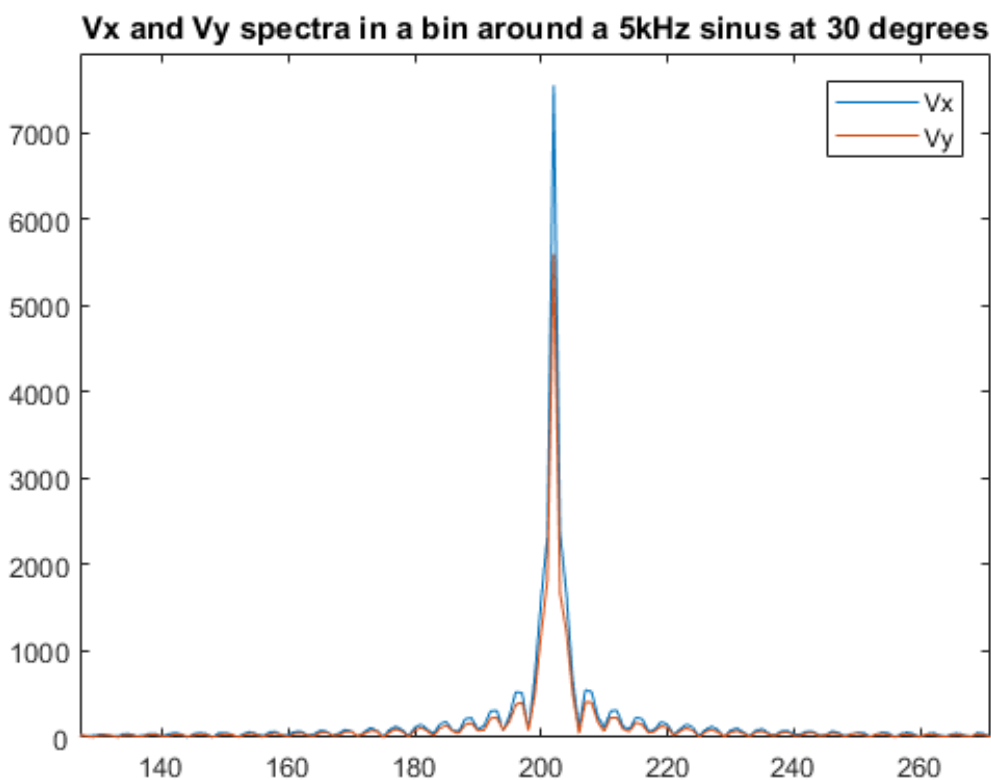


**Figure 3-2:** Spectra of  $v_x$  and  $v_y$  in a bin of  $\pm 20 Hz$  around 5kHz

### 3-3 Simulation

In order to validate the proposed methods simulations have been made. The simulation is based upon the data model given in Chapter 2. The simulated noise is uncorrelated white Gaussian noise. For both the Time- and Frequency-domain approach a pulse (see Figure 3-3) and a sinusoidal signal (see Figure 3-6) have been simulated at a DOA of 80 degrees. And is sampled at a samplefrequency of  $16kHz$ .

The simulation plotted the results of both the DOA estimation techniques with respect to impulse length  $N$  ranging from 1 to 16000 *samples* and to the signal to noise ratio's ranging between  $-30dB$  and  $10dB$ .

#### 3-3-1 Simulation with an impulse signal

The result for the time-domain approach can be found in Figure 3-4(a) and the result for the frequency-domain approach can be found in Figure 3-4(b). Since one of the requirements is to have a maximum deviation of  $\pm 5^\circ$ , Figures 3-5(a) and 3-5(b) show when the approaches have a maximum deviation of  $\pm 5^\circ$ .

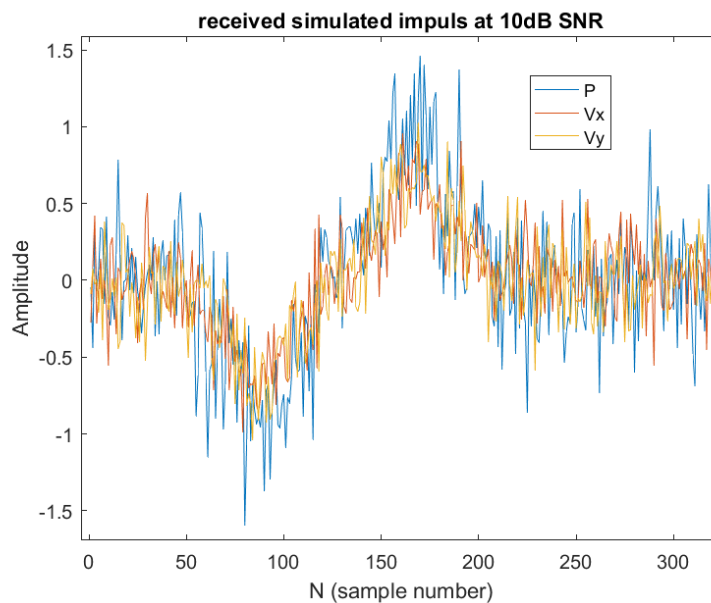


**Figure 3-3:** The received simulated impulse signal with a signal to noise ratio of 10dB. The signal is present from sample  $\pm 50$  to sample  $\pm 200$ . The sample-frequency is  $16kHz$ .

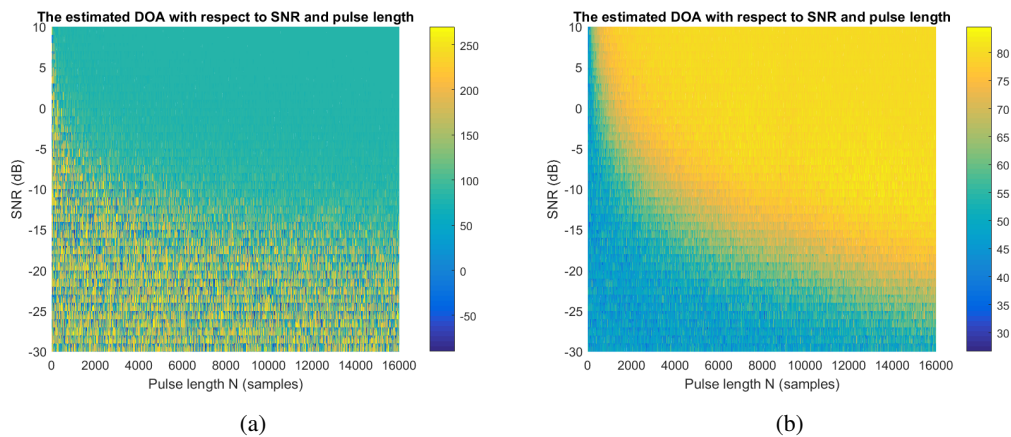


**Figure 3-4:** The estimated DOA of a source at 80 degree with respect to SNR(dB) and impulse length N(samples) using the Time- (a) and Frequency-domain (b) approach.

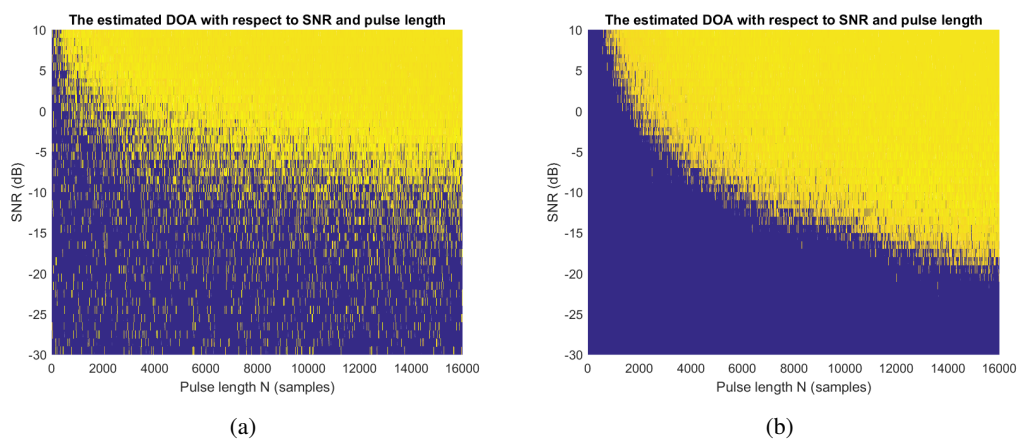


**Figure 3-5:** The estimated DOA of a source at 80 degree with respect to SNR(dB) and impulse length N(samples) using the Time- (a) and Frequency-domain (b) approach, the yellow domain indicates a maximum deviation of  $\pm 5^\circ$ .

### 3-3-2 Simulation with a sinusoidal signal

The result for the time-domain approach can be found in Figure 3-7(a) and the result for the frequency-domain approach can be found in Figure 3-7(b). Since one of the requirements is to have an accuracy of  $\pm 5^\circ$ , Figures 3-8(a) and 3-8(b) show when the approaches have a maximum deviation of  $\pm 5^\circ$ .

Sound localization using an array of Acoustic Vector Sensors

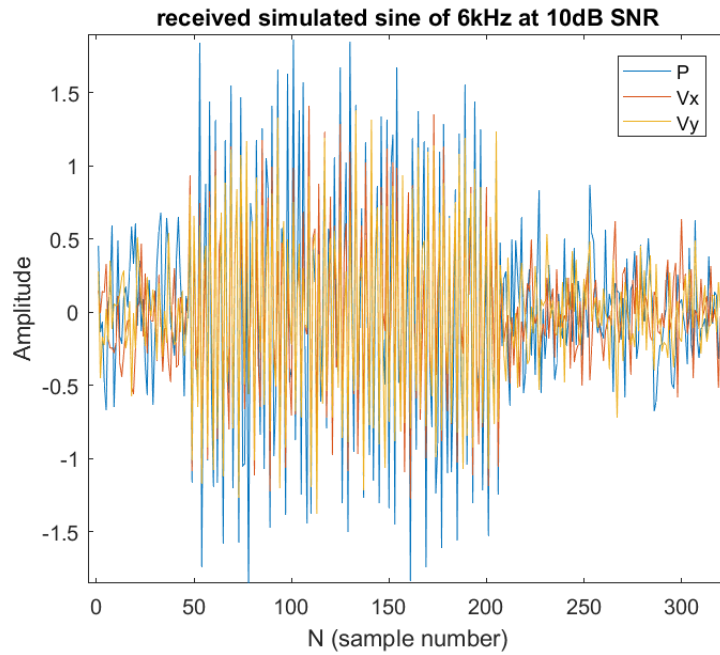


**Figure 3-6:** The received simulated sinusoidal signal with a carrier-frequency of 6kHz and with a signal to noise ratio of 10dB. The signal is present from sample  $\pm 50$  to sample  $\pm 200$ . The sample-frequency is  $16kHz$ .

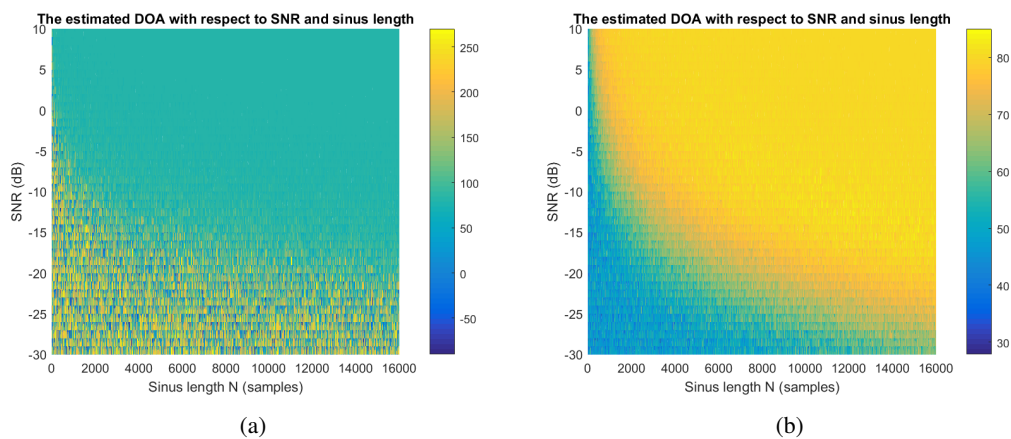


**Figure 3-7:** The estimated DOA of a source at 80 degree with respect to SNR(dB) and sinusoidal signal length N(samples) using the Time-domain (a) and Frequency-domain (b) approach.

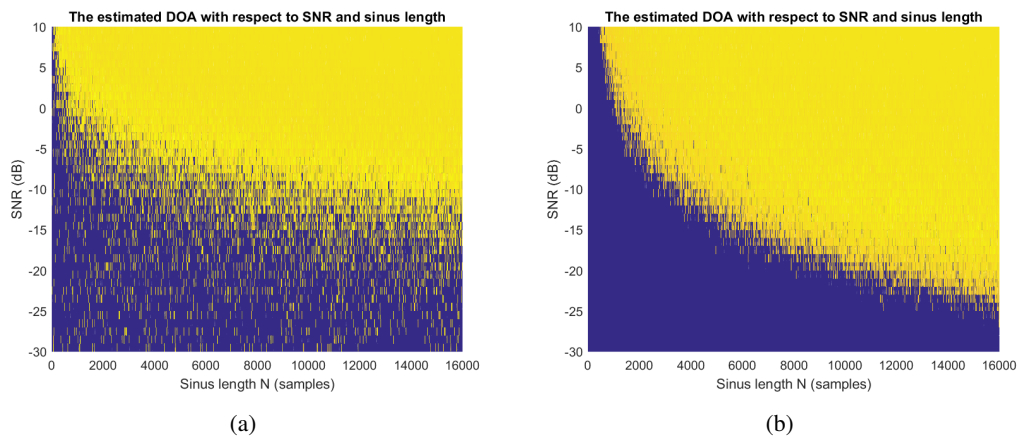


**Figure 3-8:** Estimated DOA with respect to SNR and sinus signal length for the Time- (a) and Frequency-domain (b) approach, here the yellow area indicates a a maximum deviation of  $\pm 5^\circ$

### 3-4 Discussion

The simulations of the single AVS based DOA estimation approaches show what signal length is necessary per signal to noise ratio for the approach to be useful. One requirement is that main station has to be able to locate signals with a SNR of  $-2dB$  and higher. The needed signal lengths for this requirement to be fulfilled can be found in table 3-1. Here the signal lengths  $N$  (samples) are converted to length (milliseconds), knowing that the samplefrequency of the simulation is  $16kHz$ .

**Table 3-1:** The needed signal length in milliseconds per approach

Approach:	Intrinsic TD estimation	Intrinsic FD estimation
<b>Impulse signal</b>		
Needed signal length $t$ (milliseconds):	$\geq 500$	$\geq 250$
<b>Sinusoidal signal</b>		
Needed signal length $t$ (milliseconds):	$\geq 312$	$\geq 169$

For an impulse signal the proposed time-domain approach needs 500 milliseconds of signal to be useful for DOA estimation. The frequency-domain approach needs 250 milliseconds of signal for DOA estimation. For a sinusoidal signal the results are slightly better. The time-domain approach needs 312 milliseconds of signal for an accurate DOA estimation. The frequency-domain approach needs 169 milliseconds of signal for an accurate DOA estimation of a sinusoidal signal. This means that an impulse needs to be of a minimum length of 250 milliseconds for DOA estimation using a single AVS. A sinusoidal signal needs to be of a minimum length of 169 milliseconds for DOA estimation using a single AVS.

---

# Linear phased array based DOA estimation

Before AVSs became available it was necessary to use an array of pressure sensors to determine the direction towards the source of a signal. Multiple DOA algorithms have been developed already for this type of array. Examples are among others TDOA [3] and several types of beamforming [4].

Since the Nyquist spatial sampling theorem states that the distance between the microphones needs to be at least half of the wavelength of the measured signal, this type of array becomes rather large for low-frequency signals. This relation can be seen in Equation 4-1 [17] where  $\lambda$  is the signal's wavelength,  $c$  is the speed of sound in the relative medium (In air being  $340m/s$ ), and  $f$  is the signal's frequency. For example, to detect a signal at  $1kHz$  (Wavelength of  $34cm$ ), the distance between each microphone must be at least  $17cm$ .

$$d = \frac{\lambda}{2} = \frac{c}{2f} \quad (4-1)$$

As seen in [16], an AVS array does not have this problem as the velocity gain modulation term of the beam pattern does not depend on the frequency of the source signal or amount of sensors in the array. This means that the AVS array can properly detect low-frequency sources despite the sensors being close together, which makes it possible to get a higher performance out of a smaller array.

For this thesis a linear array was used consisting of three AVS's, with  $5cm$  in between as shown in Chapter 2, making the *design-frequency* (the minimum frequency at which no spatial filtering occurs)  $3400Hz$ . This choice was made mostly because of the computational ease of a 1D array. Furthermore as shown in [18], the advantage of using AVS's over regular pressure sensors is especially noticeable in linear or planar arrays with a low amount of sensors.

In this section a TDOA implementation will be made that only uses pressure data and two beamforming algorithms, DAS and MVDR, will be adapted to use both the pressure and vector data. The resulting algorithms will again be simulated for both sinusoidal- and for impulse-signals. This will be done with varying SNR and signal length after which the accuracy will be determined for each combination.

## 4-1 Time Delay Of Arrival

Time Delay Of Arrival (TDOA) is a common way of detecting the DOA of a source with regular pressure sensors. Since AVS's also contain a pressure sensor this algorithm will be explored for comparison.

Due to the distance between the sensors in an array combined with the finite speed of sound, a time delay will occur between when an acoustic signal arrives at each microphone. Under the far-field assumption, i.e. when the acoustic wave can be modeled as a straight line, this delay is easily translated to an angle: When the wave arrives perpendicular to the array this delay will be zero, whereas when the signal arrives parallel to the array this delay will reach a maximum. This delay can be found by taking the cross-correlation of the output signals of the microphones [3]. Since these signals are highly correlated as they consist mostly of the same acoustic signal, there will be strong peaks in the cross correlation of these signals. As can be seen in Figure 4-1 these peaks will be shifted based on the DOA.

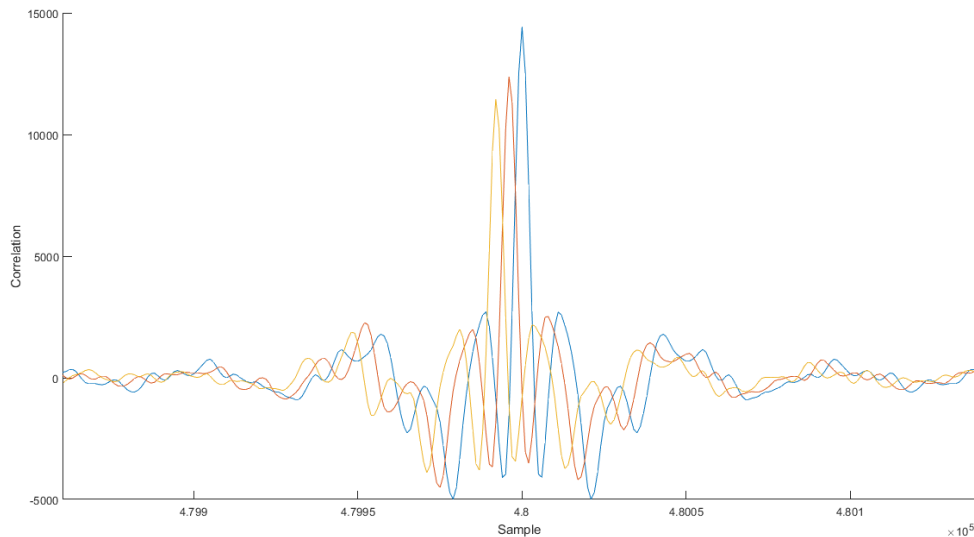


**Figure 4-1:** Shift in correlation-peak between the outputs of a 3 microphone linear array. DOA is 60 degrees, the spacing between microphones is 5cm and the samplerate is 48kHz

This shift in time can be translated to the extra distance the acoustic wave had to travel, which in turn can be used to find the angle of arrival as seen in Equation 4-2 where  $\phi$  is the angle of arrival,  $\Delta t$  is the time delay as obtained from the shift in correlation,  $c$  is the speed of sound and  $d$  is the distance between the microphones in a linear array.

$$\phi_{DOA} = \arccos \frac{\Delta t * c}{d} \quad (4-2)$$

The downsides of TDOA however are that it cannot distinguish multiple sources and will calculate a DOA based on the location of each source combined. Furthermore when, especially at low SNR,

one sensor fails to properly detect the signal, the accuracy of the entire array is lost [2]. Finally, a linear array of solely pressure sensors is unable to distinguish a signal reaching it from 'above' or 'below' the array's axis [18].

## 4-2 Beamforming

Beamforming is another technique where the direction of arrival of a signal can be retrieved by using a linear phased array of sensors. It is usually done in the frequency domain because of its advantages in comparison with time domain beamforming [19]. The goal of beamforming is to estimate the directions of the sources as those that maximize the output power of the beamformer when pointing in a scanning direction  $\phi$  [20].

The two beamforming methods considered are Delay and Sum (DAS) beamforming and Minimum Variance Distortion Response (MVDR) beamforming (also known as Capon beamforming). These two methods were chosen to work with because they don't need statistical properties of the received data [17] and are therefore useful for the direction of arrival estimation of sound signals of which these properties are unknown. Also the amount of sources in the received signal does not need to be known in advance. MVDR beamforming has the advantage of being capable of distinguishing multiple near-located sources because it suppresses sound sources in the directions it is not pointing at, while maintaining a unit gain towards this DOA [21].

The DAS beamforming spectrum can be found using Equation 4-3 [20].

$$DAS_{power}(\hat{\phi}) = \frac{a^H(\hat{\phi})Ra(\hat{\phi})}{a^H(\hat{\phi})a(\hat{\phi})} \quad (4-3)$$

The MVDR beamforming spectrum can be found using Equation 4-4 [20].

$$MVDR_{power}(\hat{\phi}) = \frac{1}{a^H(\hat{\phi})R^{-1}a(\hat{\phi})} \quad (4-4)$$

Where  $R$  is the covariance matrix of the FFT of the received signal  $s(t)$  of Equation 2-7 and  $a(\hat{\phi})$  is the *steering vector*. A steering vector describes the propagation delays between the receiving AVSs of a signal wave coming from a direction  $\phi$ . The steering vector is used to scan in between a range of angles  $\hat{\phi} = [\hat{\phi}_a \ \hat{\phi}_b]$  using the data model found in Equation 2-5 and Equation 2-7. For a far-field source signal received on a AVS array of length  $M$  the steering vector can be represented as in Equation 4-5.

$$a(\hat{\phi}) = \begin{bmatrix} \begin{bmatrix} \frac{1}{\rho c} \\ \cos \hat{\phi} \\ \sin \hat{\phi} \end{bmatrix} \\ e^{i*k*d*\cos \hat{\phi}} \begin{bmatrix} \frac{1}{\rho c} \\ \cos \hat{\phi} \\ \sin \hat{\phi} \end{bmatrix} \\ \vdots \\ e^{i*k*(M-1)*d*\cos \hat{\phi}} \begin{bmatrix} \frac{1}{\rho c} \\ \cos \hat{\phi} \\ \sin \hat{\phi} \end{bmatrix} \end{bmatrix} \in \mathbb{C}^{3M \times 1} \quad (4-5)$$

When a scan is made between  $\phi_a$  and  $\phi_b$  the spectrum can be drawn. An example of such a spectrum in a polar coordinate system can be seen in Figure 4-2. In this case the scan was made between  $\phi_a = 90$  and  $\phi_b = 180$ . The DOA can be estimated by taking the  $\hat{\phi}$  at which the power output reaches a maximum value. In the case of Figure 4-2 this would be 125 degrees for both MVDR and DAS. When multiple sound sources are present in the incoming signal  $s(t)$  there will be multiple distinct peaks in the spectrum corresponding to these sources. An example is shown in Figures 4-3(a) and 4-3(b).

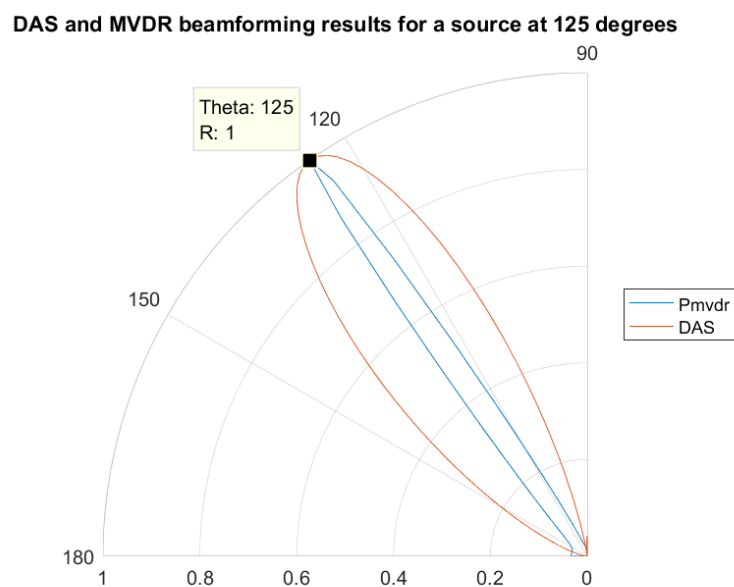
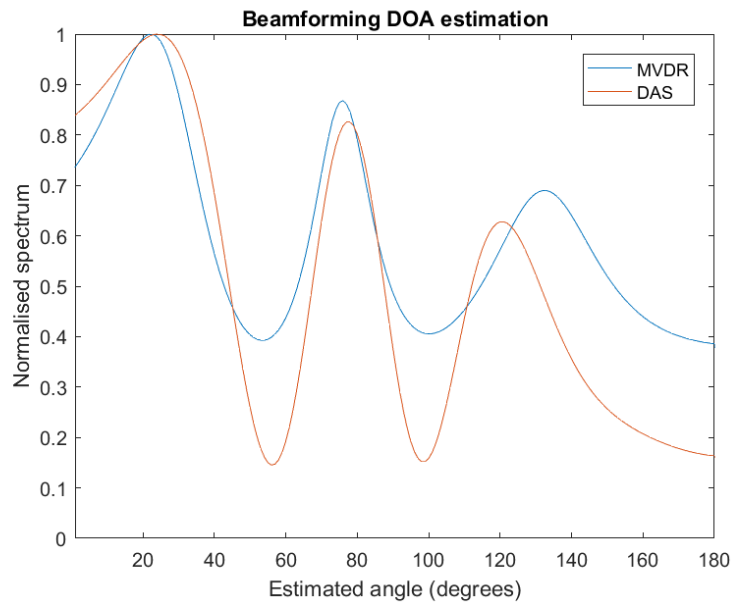
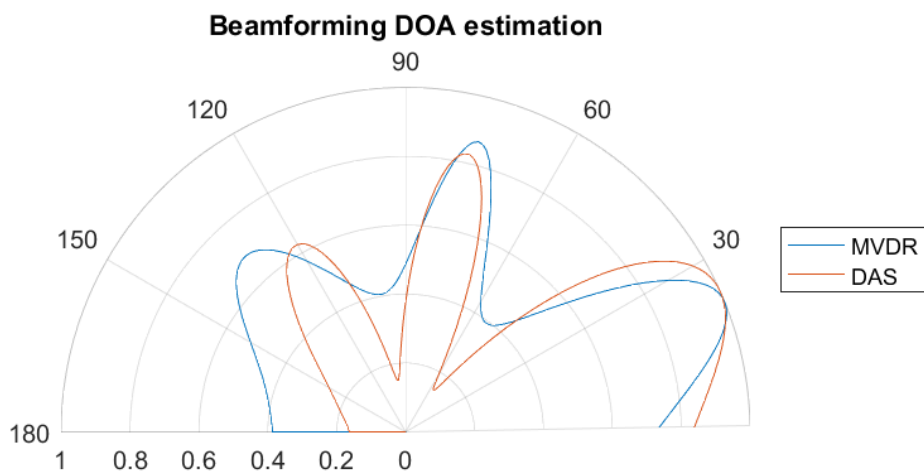


**Figure 4-2:** The beamforming spectra of MVDR and DAS for a single source located at 125 degrees

Sound localization using an array of Acoustic Vector Sensors



(a)



(b)

**Figure 4-3:** DAS and MVDR spectra represented in cartesian (a) and (b) polar coordinate systems, sound sources are located at  $\phi = 15^\circ$ ,  $\phi = 75^\circ$  and  $\phi = 135^\circ$ .



### 4-3 Simulation

As was the case for the intrinsic algorithms, simulations have been performed with each of the mentioned array-algorithms. The simulation is based upon the data model given in Chapter 2. The simulated noise is uncorrelated white Gaussian noise. For both TDOA and beamforming an impulse (see Figure 3-3) and a sinusoidal signal (see Figure 3-6) have been simulated with a DOA of  $125^\circ$ . And is sampled at a samplefrequency of  $16kHz$ .

The simulation plotted the results of both the DOA estimation techniques with respect to impulse length  $N$  ranging from 1 to 16000 *samples* and to the signal to noise ratio's ranging between  $-30dB$  and  $10dB$ .

#### 4-3-1 TDOA

The result for the TDOA approach can be found in Figures 4-4(a) to 4-5(b). In Figures 4-4(a) and 4-4(b) the DOA estimations of an impulse and sinus can be found. Since one of the requirements is to have a accuracy of  $\pm 5^\circ$ , Figures 4-5(a) and 4-5(b) show when TDOA has a maximum deviation of  $\pm 5^\circ$ .

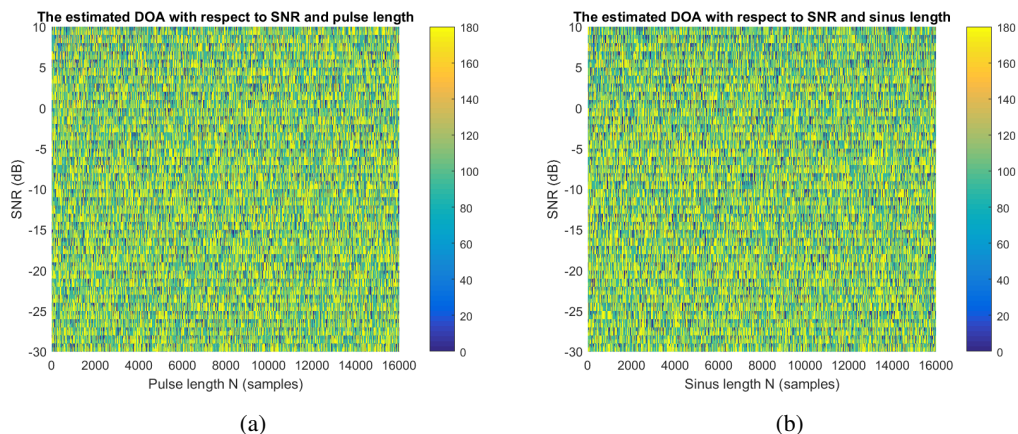


**Figure 4-4:** Estimated DOA by TDOA with respect to SNR and signal length for an impulse (a) and a sine (b)

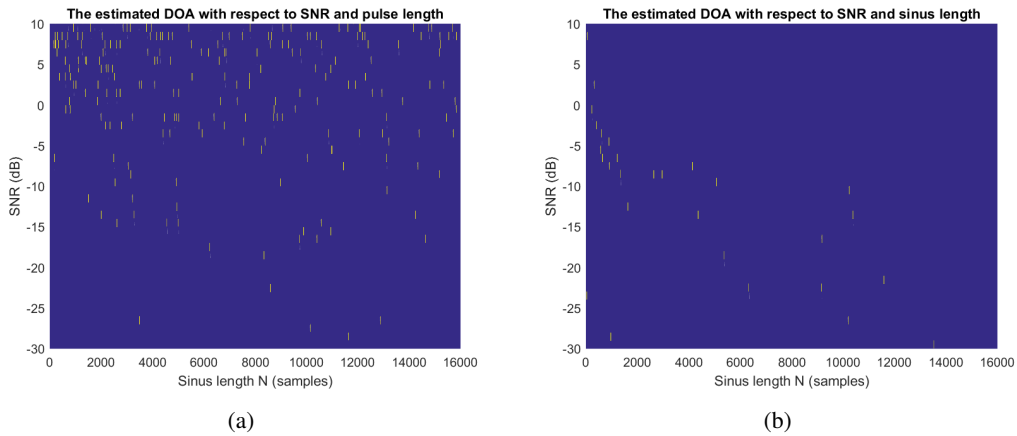


**Figure 4-5:** Estimated DOA by TDOA with respect to SNR and signal length for an impulse (a) and a sine (b), here the yellow area indicates a maximum deviation of  $\pm 5^\circ$ .

### 4-3-2 Beamforming

Firstly sources with carrierfrequencies from  $1Hz$  to  $8kHz$  at different SNRs were simulated. The results of this simulation can be found in Figures 4-6(a) and 4-6(b). Secondly the DOA estimations for both the beamforming techniques were simulated for a signal of different SNRs and lengths as explained in Section 4-3. The results for the DAS and MVDR beamforming approaches can be found in Figures 4-7(a) to 4-10(b).

The beamforming results for an impulse signal can be found in Figures 4-7(a) and 4-7(b). Where Figures 4-8(a) and 4-8(b) denote when the beamformers have a maximum deviation of  $\pm 5^\circ$  for an impulse signal. The beamforming results for a sinusoidal signal can be found in Figures 4-9(a) and 4-9(b). Where Figures 4-10(a) and 4-10(b) show when the beamformers have a maximum deviation of  $\pm 5^\circ$  for a sinusoidal signal.

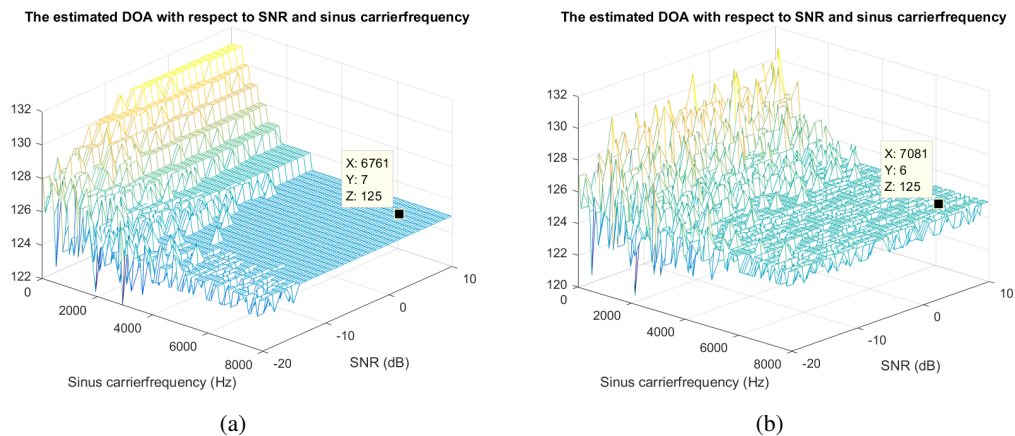


**Figure 4-6:** Estimated DOA with respect to SNR and sinusoidal signal of different carrier-frequencies for DAS (a) and MVDR (b) beamforming

Sound localization using an array of Acoustic Vector Sensors

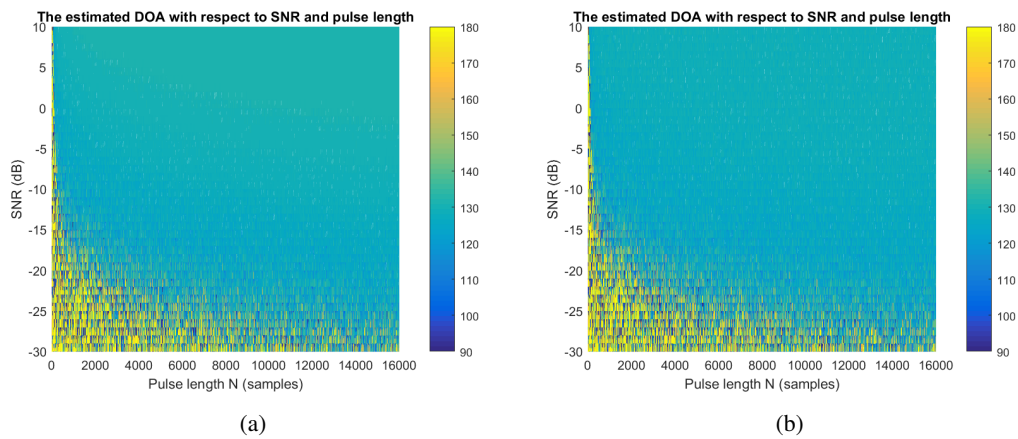


**Figure 4-7:** Estimated DOA with respect to SNR and impulse signal length for DAS (a) and MVDR (b) beamforming

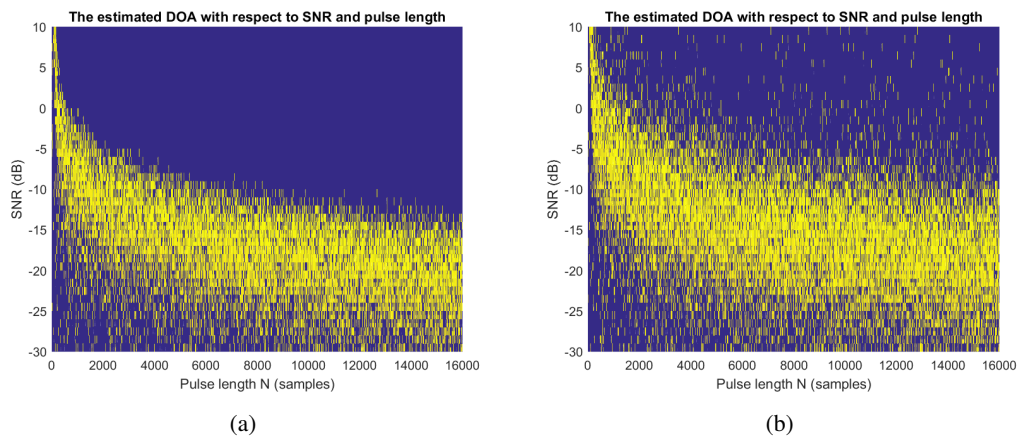


**Figure 4-8:** Estimated DOA with respect to SNR and impulse signal length for DAS (a) and MVDR (b) beamforming, here the yellow area indicates a maximum deviation of  $\pm 5^\circ$ .

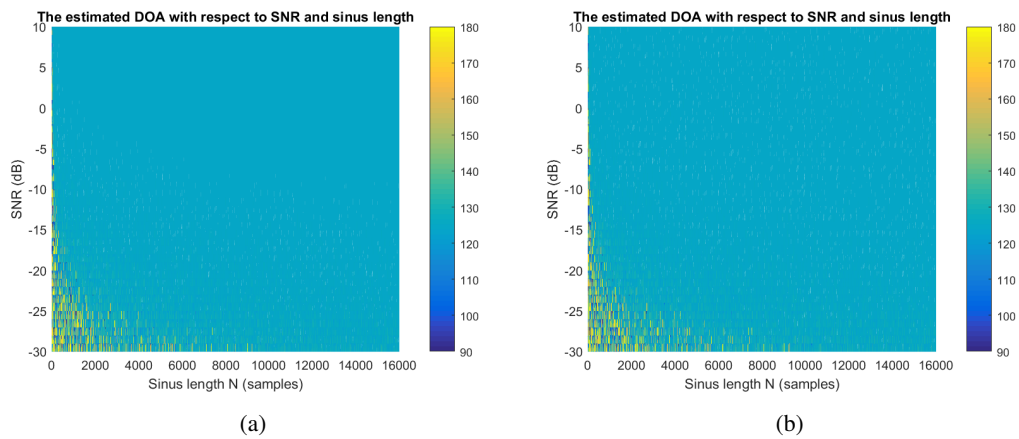


**Figure 4-9:** Estimated DOA with respect to SNR and sinus signal length for DAS (a) and MVDR (b) beamforming

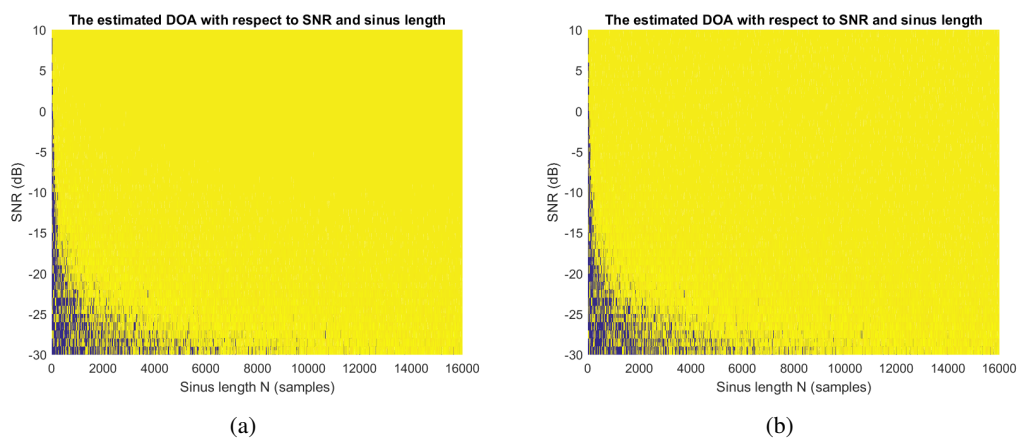


**Figure 4-10:** Estimated DOA with respect to SNR and sinus signal length for DAS (a) and MVDR (b) beamforming, here the yellow area indicates a maximum deviation of  $\pm 5^\circ$ .

## 4-4 Discussion

The statement that an AVS array can properly detect low frequency sources [16] was tried to be validated by Figures 4-6(a) and 4-6(b). This statement seems to hold, however, the design-frequency still has an effect on the accuracy of the estimated angle when the carrier frequency drops below this design-frequency. This effect being a maximum deviation of  $6^\circ$  at an SNR of  $0dB$ , does make an AVS array useful for beamforming low frequency signals.

The simulations of the linear phased AVS array based DOA estimation approaches show what signal length is necessary per signal to noise ratio for the approach to be useful. One requirement is that main station has to be able to locate signals with a SNR of  $-2dB$  and higher. The needed signal lengths for this requirement to be fulfilled can be found in Table 4-1. Here the signal lengths  $N$  (samples) are converted to length  $t$  (milliseconds), knowing that the sample frequency of the simulation is  $16kHz$ .

**Table 4-1:** The needed signal length per approach

Approach:	TDOA	DAS beamforming	MVDR beamforming
<b>Impulse signal</b>			
Needed signal length $t$ (milliseconds):	X	$9.4 \leq t \leq 12.5$	$6.3 \leq t \leq 18.8$
<b>Sinusoidal signal</b>			
Needed signal length $t$ (milliseconds):	X	$t \geq 12.5$	$t \geq 12.5$

TDOA showed to be useless in simulation. The most likely explanation is that the noise used in the simulation is uncorrelated for each of the AVSs, which caused the calculated correlation shift to be wrong. Another problem could be the impulse model used for the simulation, however that model did hold up for the other simulations. Therefore the table has been left blank regarding the TDOA approach. Later on in this report TDOA will be tested with measurements.

Noticeable from the plots is the lack of accuracy for the beamforming algorithms when the received signal is an impulse. Which makes sense since the beamforming algorithm are performed in the frequency domain and impulses don't have a distinct carrier frequency.

Beamforming however does have an excellent accuracy for sinusoidal signals. The signal does only have to be around 12.5 milliseconds long for the beamforming algorithms to hit a accuracy of  $\pm 5^\circ$ . This means that estimating the DOA of an impulse should not be done using beamforming. Data containing a sinusoidal signal needs to be of a minimum length of 12.5 milliseconds for DOA estimation using an AVS array.

---

# Results

In this chapter the DOA estimation techniques discussed in this report are applied to real measurements. To do this first a measurement setup was made which corresponds to the theoretical setup used in the simulations of Chapters 3 and 4. This setup is explained in Section 5-1. The DOA estimation results of the done measurements are given in Section 5-2.

## 5-1 Measurement setup

The measurement setup used to test the DOA estimation techniques consist of 3 linearly spaced acoustic vector sensors along the negative x-axis. With a spacing of  $d = 0.05m$ . Both sinusoidal and impulse signals were produced and recorded.

Three types of sinusoidal signals were created with carrier frequencies of  $1kHz$ ,  $3kHz$  and  $5kHz$ . To generate these signals a loudspeaker was used located at angles of  $\phi = 30^\circ$ ,  $\phi = 45^\circ$  and  $\phi = 60^\circ$  with respect to the positive x-axis. This placement is chosen to maximize the effect of far-field sources since the distance at which the sources could be placed was limited to  $r = 1.5m$ . The real setup can be seen in Figure 5-1, a visual representation in Figure 5-2.

Since the available software at the test location could not play impulses, these signals were made by hand. This was done by hitting a screwdriver against the steel leg of a chair. As with the speakers this was repeated at angles of  $\phi = 30$ ,  $\phi = 45$  and  $\phi = 60$  degrees. For clarity only a selection of the sinusoidal signals is discussed in this report. An overview of the signals of which the results will be discussed can be seen in Table 5-1.

**Table 5-1:** Generated and recorded signal types

Signal type:	Recording 1	Recording 3	Recording 3
Sine wave	$f=1kHz$ , $\phi = 45^\circ$ , $SNR = 0.1dB$	$f=3kHz$ , $\phi = 30^\circ$ , $SNR = 0.9dB$	$f=5kHz$ , $\phi = 60^\circ$ , $SNR = 1.8dB$
Impulse	$\phi = 30^\circ$ , $SNR \approx 4dB$	$\phi = 45^\circ$ , $SNR \approx 4dB$	$\phi = 60^\circ$ , $SNR \approx 4dB$

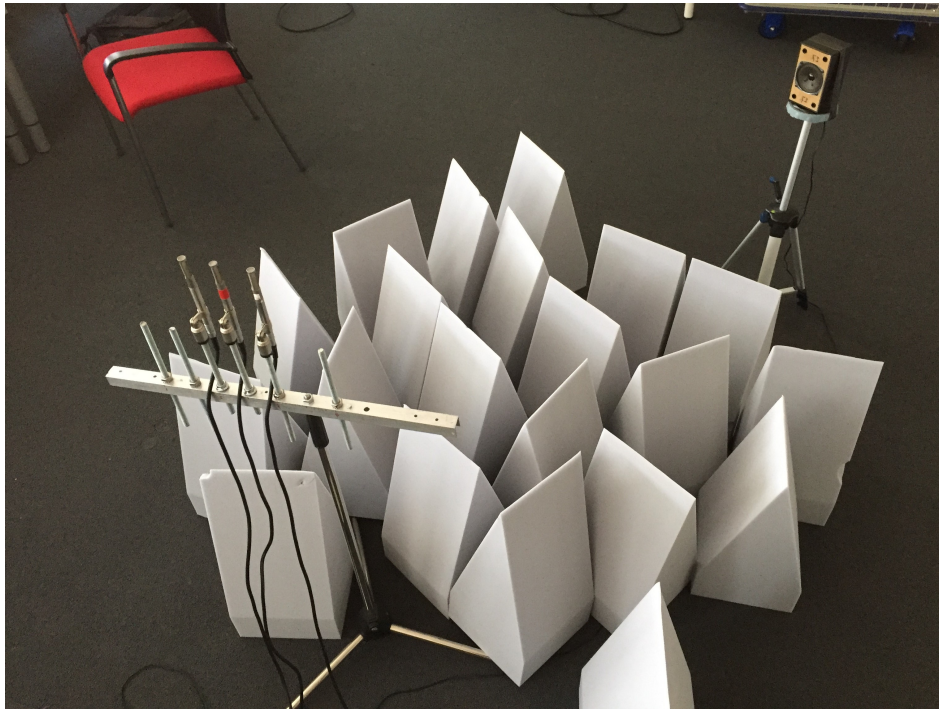


**Figure 5-1:** The measurement setup

Sound localization using an array of Acoustic Vector Sensors

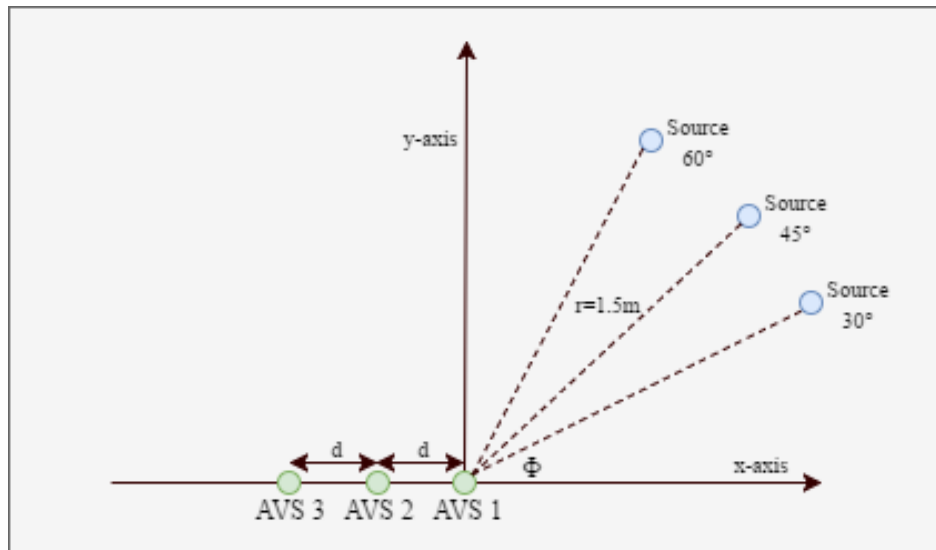


**Figure 5-2:** A visual representation of the measurement setup used

## 5-2 Measurement results

To simulate the way the mainstation would receive the data in real use the recordings were split in smaller sections to represent packages. To find the minimum amount of data needed for an algorithm to find an accurate DOA, packages of sizes 24000, 12000, 6000, 3000 and 600 samples were tried, corresponding with  $\frac{1}{2}^{th}$ ,  $\frac{1}{4}^{th}$ ,  $\frac{1}{8}^{th}$ ,  $\frac{1}{16}^{th}$  and  $\frac{1}{80}^{th}$  of a second of data respectively. To improve the results and remove some of the noise, the results of the algorithms were passed through a basic 1D Kalman filter based off of [22] if needed.

### 5-2-1 Intrinsic

Both intrinsic algorithms performed similarly for detecting sinusoidal signals. A plot of the output of the frequency-domain implementation after filtering can be seen in Figure 5-3. The results can be seen in Table 5-2. Both algorithms retained this same performance down to 600 samples per calculation.

The results of the time-domain implementation with impulse signals are shown in Table 5-3. A plot of impulses at 60 degrees is given in Figure 5-4. The package size was kept at 6000 as no valid result was achieved under that. The calculations were only updated when an impulse was present for clarity and no Kalman filter was applied. The frequency-domain intrinsic implementation did not result in any valid estimations no matter the package size.

**Table 5-2:** Intrinsic DOA of sinusoidal signals

Algorithm	$f = 1kHz$ at 45 degrees	$f = 3kHz$ at 30 degrees	$f = 5kHz$ at 60 degrees
Time	60 degrees $\pm$ 3	20 degrees $\pm$ 3	65 degrees $\pm$ 3
Frequency	60 degrees $\pm$ 3	21 degrees $\pm$ 3	59 degrees $\pm$ 3

**Table 5-3:** Time domain intrinsic DOA of impulse signal

Impulse at 30 degrees	Impulse at 45 degrees	Impulse at 60 degrees
25 degrees $\pm$ 8	42 degrees $\pm$ 8	60 degrees $\pm$ 8

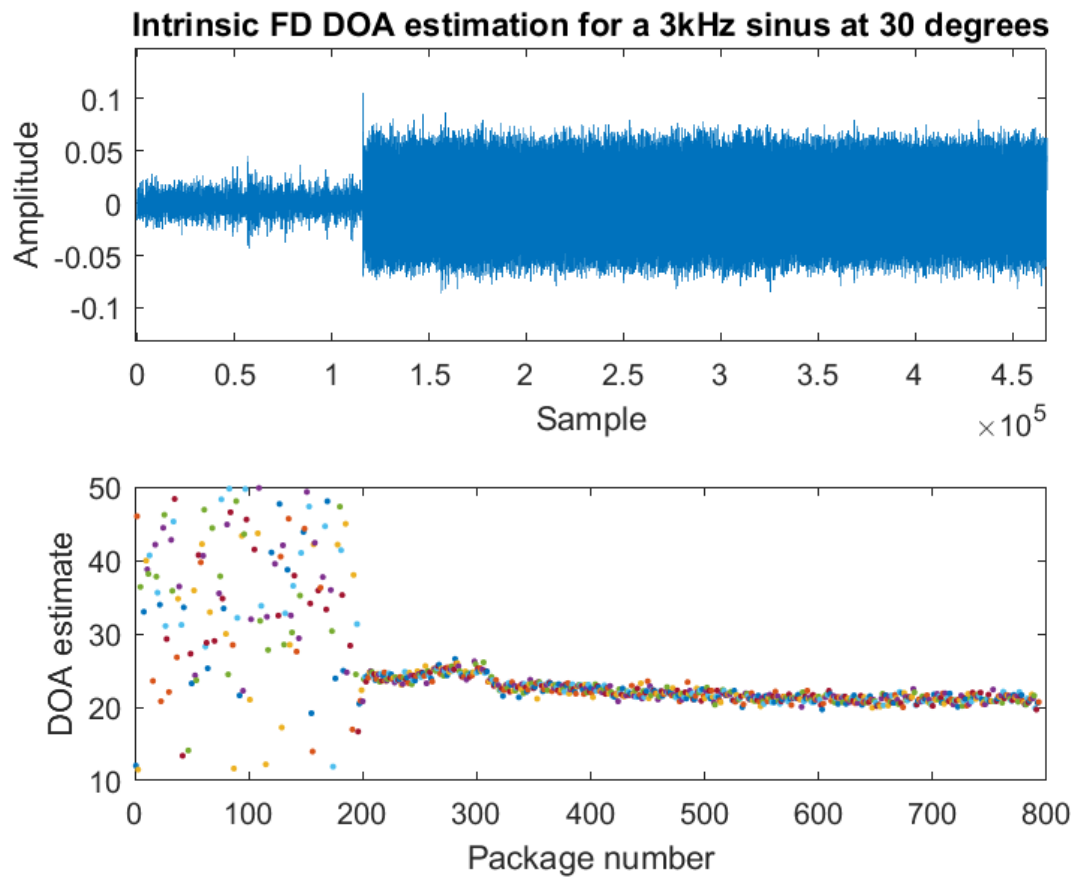


**Figure 5-3:** DOA from frequency domain intrinsic algorithm. Package size 600 samples,  $f = 3kHz$  at 30 degrees

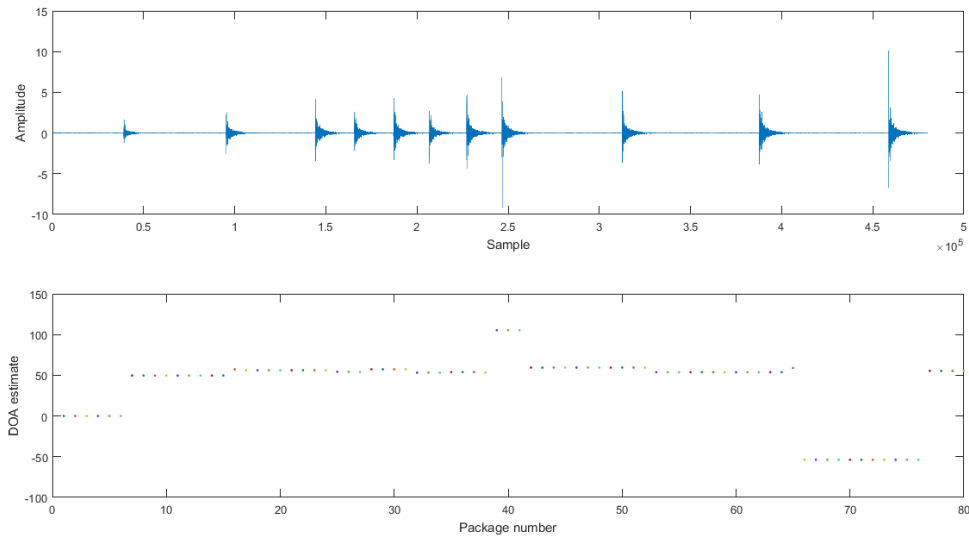


**Figure 5-4:** DOA from time domain intrinsic algorithm. Package size 6000 samples, impulses at 60 degrees

### 5-2-2 TDOA

TDOA could not detect the DOA of any sinusoidal signal for any package size. The results always converged to either 0 or 180 degrees. An example of this is shown in Figure 5-5.

The results of an impulse signal can be seen in Table 5-4. An example of one such signal and its DOA estimation is shown in Figure 5-6. As was the case with the intrinsic impulse plot the DOA was only updated when an impulse was present and no Kalman filtering was applied to the output signal. Impulse detection worked with few outliers of up to  $\pm 50$  degrees down to 6000 samples per calculation.

**Table 5-4:** TDOA DOA of impulse signals

Impulse @ 30 degrees	Impulse at 45 degrees	Impulse at 60 degrees
31 degrees, 4 outliers	44 degrees, 1 outlier	55 degrees, 2 outliers

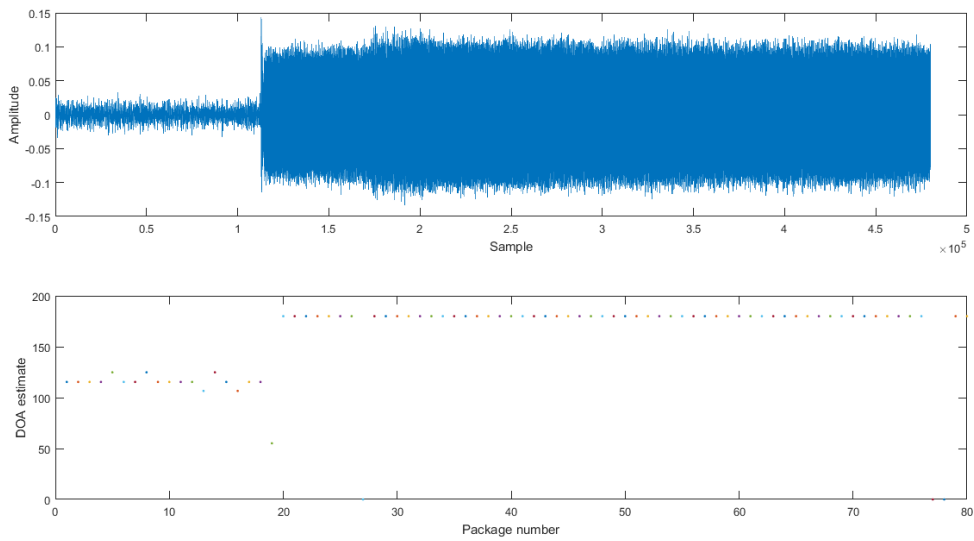


**Figure 5-5:** DOA from TDOA algorithm for a sinus  $f = 5kHz$  at 60 degrees, package size 6000 samples

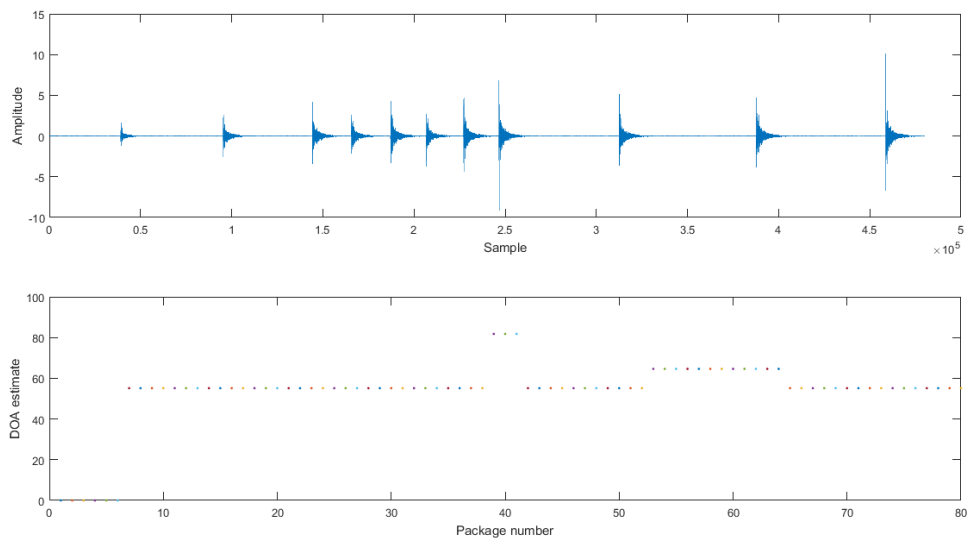


**Figure 5-6:** DOA from TDOA algorithm for an impulse signal at 60 degrees, package size 6000 samples

### 5-2-3 Beamforming

The results of the Delay And Sum algorithm when measuring sinusoidal signals can be seen in Table 5-5. DAS maintains this accuracy down to packages of 600 samples. An example of this performance can be seen in Figure 5-7. MVDR did not lead to any usable results, even when filtered with the

Sound localization using an array of Acoustic Vector Sensors

Kalman filter and on packages of 24000 samples (Half a second). An example of this can be seen in Figure 5-8.

Neither DAS nor MVDR could properly detect impulses coming from 30 degrees. Impulse signals from 45 or 60 degrees were detected with several outliers by both DAS and MVDR. The results from MVDR with a signal from 60 degrees and a package size of 6000 samples can be seen in Figure 5-9. The results from the DAS implementation of the same signal can be seen in Figure 5-10.

**Table 5-5:** DAS DOA estimations at sinusoidal signals

$f = 1kHz @ 45 \text{ deg}$	$f = 3kHz @ 30 \text{ deg}$	$f = 5kHz @ 60 \text{ deg}$
38 degrees $\pm 3$	31 degrees $\pm 2$	51 degrees $\pm 3$

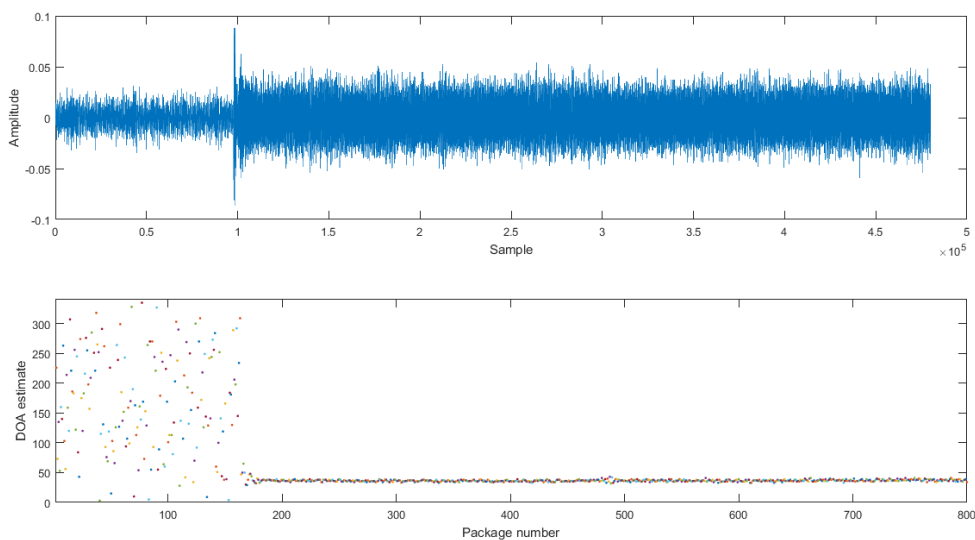


**Figure 5-7:** DAS output for a sinusoidal signal  $f = 1kHz$  at 45 degrees, package size 600 samples

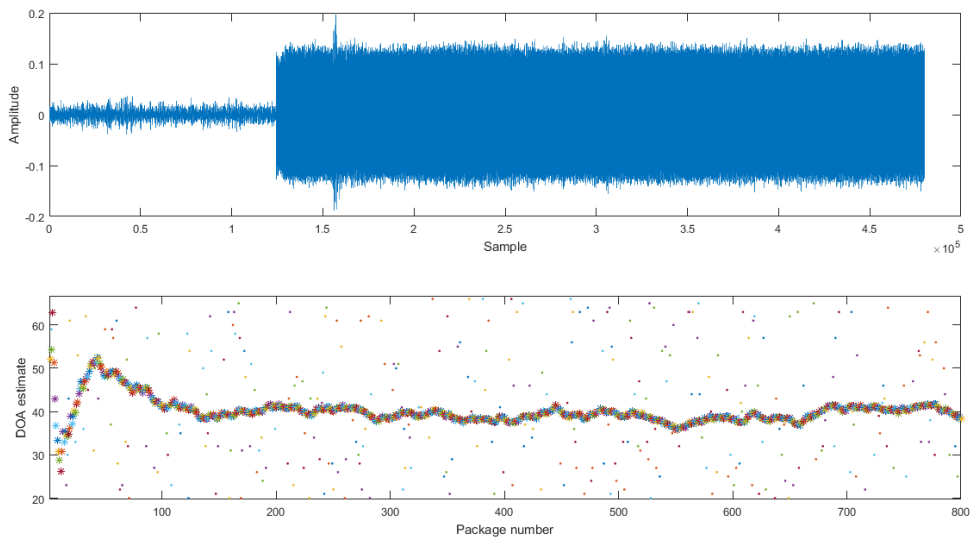


**Figure 5-8:** MVDR DOA estimation of a  $f = 5kHz$  sinusoidal source at 30 degrees, as well as the result after applying the Kalman filter.

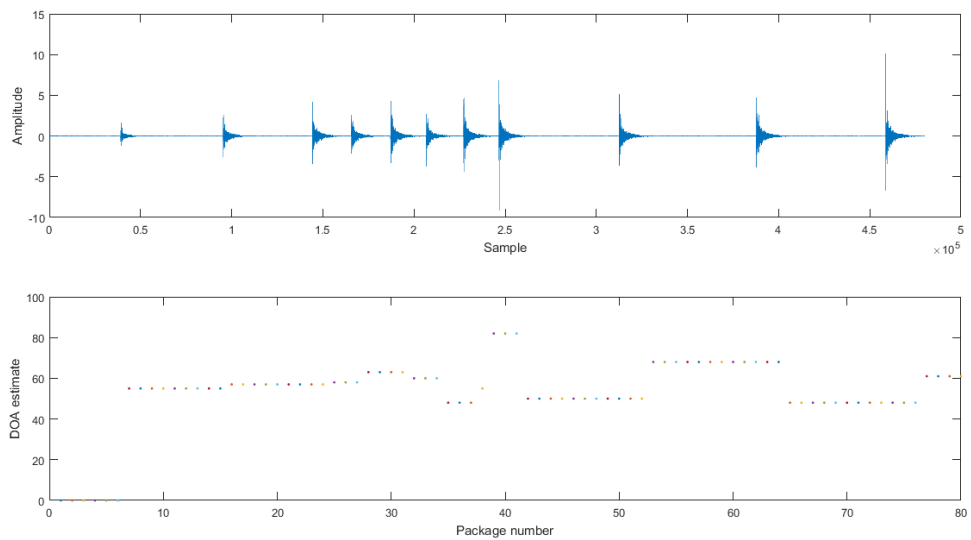


**Figure 5-9:** MVDR DOA estimation of impulse signal originating from 60 degrees with a package size of 6000 samples

Sound localization using an array of Acoustic Vector Sensors

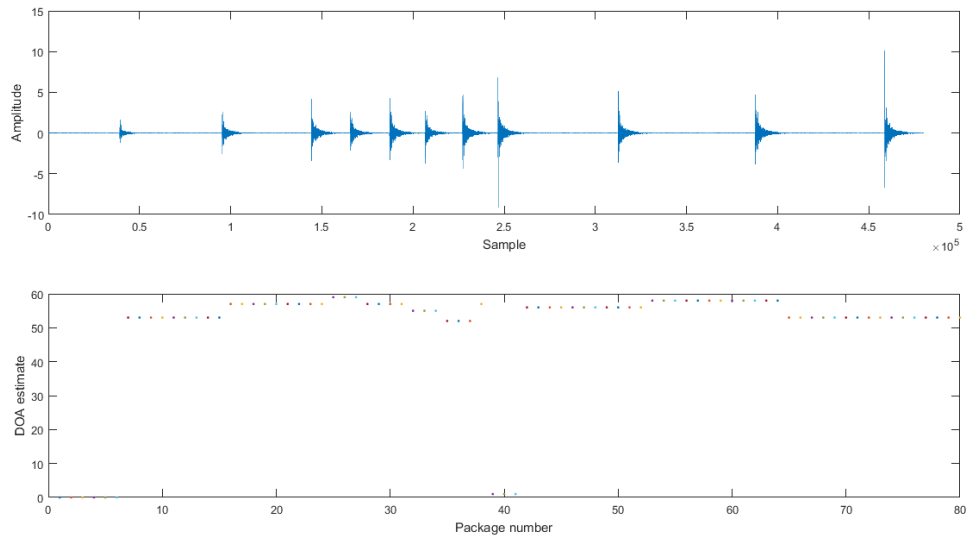


**Figure 5-10:** DAS DOA estimation of impulse signal originating from 60 degrees with a package size of 6000 samples

---

# Discussion

The measurements and their respective DOA estimations using the techniques discussed in this report give a good indication which algorithm is best for which signal type. Now these results will be discussed.

While reading this discussion, non-ideal circumstances of the measurement setup have to be kept in mind. Such as the fact that this was a rather near-field setup and there were plenty of objects around that could cause reflections. Furthermore in the actual setup the sources may not have been at exactly their intended angles which could have somewhat shifted the DOA of the signal to the sensors.

Both the Intrinsic Time-domain and Frequency-domain approach showed to be a good option for sinusoidal signals. With SNRs ranging from  $0dB$  for the  $1kHz$  sinus to  $2dB$  for the  $5kHz$  sinus, the minimum signal length needed of these measurements to be able to estimate the DOA was 600 samples. This corresponds to the simulated Figures 3-8(a) and 3-8(b). The DOA estimations for the  $1kHz$  signal were, although stable, far from the real value. This could mean the SNR of  $0dB$  of that signal was too low to be able to locate the source.

The Intrinsic Time-domain approach showed to be a good option for impulses. The minimum signal length needed for a DOA estimate is 6000 samples, which corresponds to Figure 3-5(a) for a signal of  $4dB$ . This again corresponded to the actual SNR of the used impulse signal. The Intrinsic Frequency-domain approach did not work for impulses. The reason for this is that an impulse does not have a specific carrier frequency for the algorithm to focus on.

Time Delay of Arrival would be a good option for impulse signals. The TDOA DOA results are however not significantly better than the Intrinsic Time-domain approach. This clearly indicates the added value of the vector sensors in an AVS compared to a regular microphone.

Of the beamforming approaches only Delay and Sum showed to be useful for locating a single source using the test setup. The MVDR beamformer had trouble with signal reflections in the room. A clear example of this can be seen in Figures 6-1(a) and 6-1(b); the MVDR beamformer does detect a source at  $60^\circ$  with one packet of 600 samples, but the reflections coming from  $80^\circ$  result in a higher peak in MVDR's spectrum in another packet of 600 samples of the same signal. The results of the DAS beamforming approach however are good for sinusoidal signals and considering MVDR beamforming will have less problems with reflections in scenarios as portrayed in 1-3, i.e. wide open areas,

it is expected that MVDR will also perform better in these real, far field situations. The minimum signal length needed for an accurate DOA estimation using DAS beamforming was found to be 600 samples, corresponding to the results of the simulation in Section 4-3.

Finally all calculations were performed faster than the time it took to make the measurements. The recorded signals were 10 seconds in length and a generic desktop computer was able to calculate the DOA of all the samples in the signal within 5 seconds. This includes MVDR, the most computationally heavy algorithm, down to 600 samples per package. On a generic laptop this was not always possible, however this should not be a problem for the use-cases as described in Section 1-3.

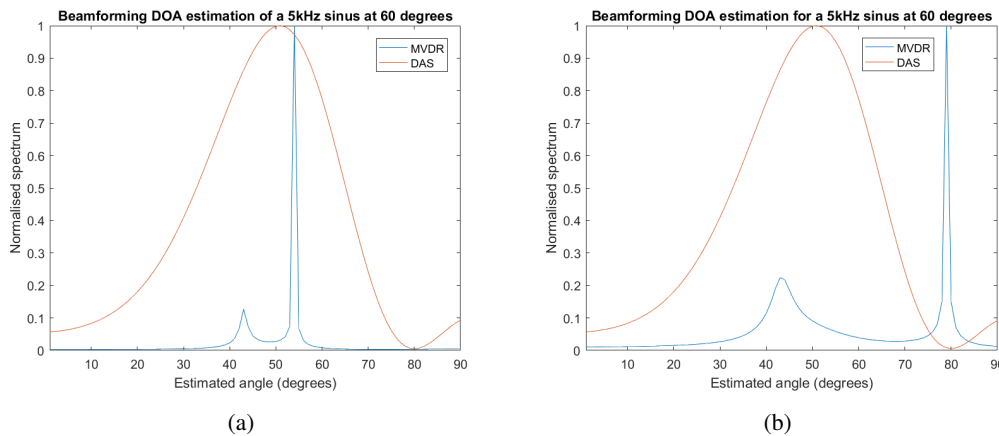


**Figure 6-1:** Two beamforming spectra of MVDR and DAS for a single source located at 60 degrees using the measurement setup

---

# Conclusion

In this report five different direction of arrival algorithms were explored for the implementation in Mainstation. The main prupose of this report was to find to most suitable DOA algorithm per signal type and signal to noise ratio.

It was found that solely using the intrinsic directionality of AVSs it is possible to get stable DOA estimates for sinusoidal signals. The results stayed within  $\pm 3$  degrees from a mean value, however this estimate was generally more than 10 degrees off from the actual DOA to the source. Impulse signals could only be detected using the intrinsic directionality in the time domain, with the mean value of the estimate laying within 5 degrees off the real value.

TDOA was found to be unusable with sinusoidal signals although the results were promising for impulses. Their mean value was within 5 degrees from the actual direction with few outliers, although it did not seem to have an advantage over the time-domain intrinsic algorithm with only one AVS.

DAS performed well for sinusoidal signals with values varying by  $\pm 3$  degrees around a mean value. This value was within 10 degrees from the actual value.

MVDR did not perform well outside of the simulations for neither sinusoidal nor impulse signals. The expected cause for this are reflections caused in the measurement-room.

Based on these results, the best suited algorithm can now be chosen from the detected signal type as provided by the array's DSP units. For impulse signals it is recommended to use the Intrinsic time domain algorithm, because this algorithm only needs one AVS to function. For sinusoidal signals the Delay and Sum beamforming algorithm is recommended.

It was found that the above results could be achieved with signal lengths of 6000 samples for impulses and down to 600 samples for sinusoidal signals at a samplerate of  $48kHz$ . The computation time was well under the required minimum when performed on a generic desktop computer; the DOA could be calculated by all algorithms faster than the time it took to collect the data.

Finally simulations showed that it was possible to determine the DOA at SNR's as low as  $-2dB$ . Real-life measurements were performed with SNR's as low as  $1dB$ .

Sound localization using an  
array of Acoustic Vector Sensors

For further development, measurements should be made in a more suitable environment. This could improve the performance of the MVDR algorithm, as well as give a more accurate representation of performance of the other algorithms. Furthermore a graphical interface could be created that shows the DOA of detected signals in real time to the user. Finally the algorithms could be optimized and written in a more low-level language than Matlab, which could allow them to be ran on portable hardware.

---

# Bibliography

- [1] J. H. DiBiase, "A high-accuracy, low-latency technique for talker localization in reverberant environments using microphone arrays," Ph.D. dissertation, Brown University, 2000.
- [2] A. L. Ramos, S. Holm, S. Gudvangen, and R. Otterlei, "Delay-and-sum beamforming for direction of arrival estimation applied to gunshot acoustics," in *SPIE Defense, Security, and Sensing*. International Society for Optics and Photonics, 2011, pp. 80 190U–80 190U.
- [3] M. Imran, A. Hussain, N. M. Qazi, and M. Sadiq, "A methodology for sound source localization and tracking: Development of 3d microphone array for near-field and far-field applications," in *Applied Sciences and Technology (IBCAST), 2016 13th International Bhurban Conference on*. IEEE, 2016, pp. 586–591.
- [4] H. Adel, M. Souad, A. Alaqeeli, and A. Hamid, "Beamforming techniques for multichannel audio signal separation," *arXiv preprint arXiv:1212.6080*, 2012.
- [5] B. Van Veen and K. Buckley, "Beamforming techniques for spatial filtering," *Digital Signal Processing Handbook*, pp. 61–1, 1997.
- [6] A. Cigada, F. Ripamonti, and M. Vanali, "The delay & sum algorithm applied to microphone array measurements: numerical analysis and experimental validation," *Mechanical Systems and Signal Processing*, vol. 21, no. 6, pp. 2645–2664, 2007.
- [7] J. Grythe, "Beamforming algorithms - beamformers," p. 1 – 5.
- [8] J. Dmochowski, J. Benesty, and S. Affes, "On spatial aliasing in microphone arrays," *IEEE Transactions on Signal Processing*, vol. 57, no. 4, pp. 1383–1395, April 2009.
- [9] M. AVISA, "Acoustic Vector Sensor," accessed 26-4-2017. [Online]. Available: <http://microflown-avisa.com/acoustic-vector-sensor>
- [10] H.-E. de Bree, "An overview of microflown technologies," *Actaacustica united withacustica*, vol. 89, p. 163 – 172, 2003.

- [11] M. Hawkes and A. Nehorai, "Surface-mounted acoustic vector-sensor array processing," in *1996 IEEE International Conference on Acoustics, Speech, and Signal Processing Conference Proceedings*, vol. 6, May 1996, pp. 3169–3172 vol. 6.
- [12] H. de Bree, "Exploring the use of the microflown," *Microflown Technologies, Twente*, 2005.
- [13] P. Se and K. Ingard, "Theoretical acoustics," 1968.
- [14] H. Chen and J. Zhao, "Coherent signal-subspace processing of acoustic vector sensor array for doa estimation of wideband sources," *Signal Processing*, vol. 85, no. 4, pp. 837 – 847, 2005. [Online]. Available: <http://www.sciencedirect.com/science/article/pii/S0165168404003305>
- [15] J. Cao, J. Liu, J. Wang, and X. Lai, "Acoustic vector sensor: reviews and future perspectives," *IET Signal Processing*, vol. 11, no. 1, pp. 1–9, 2017.
- [16] N. R. Krishnaprasad, "Acoustic vector sensor based source localization," Master's thesis, Delft University of Technology, 2016.
- [17] P. Stoica and R. Moses, "Spectral analysis of signals," *Prentice Hall*, pp. 273–280, Dec 2005.
- [18] M. Hawkes and A. Nehorai, "Acoustic vector-sensor beamforming and capon direction estimation," *IEEE Transactions on Signal Processing*, vol. 46, no. 9, pp. 1–14, Sep 1998.
- [19] U. Hamid, R. A. Qamar, and K. Waqas, "Performance comparison of time-domain and frequency-domain beamforming techniques for sensor array processing," in *Proceedings of 2014 11th International Bhurban Conference on Applied Sciences Technology (IBCAST) Islamabad, Pakistan, 14th - 18th January, 2014*, Jan 2014, pp. 379–385.
- [20] A.-J. van der Veen and G. Leus, "Signal processing for communications," *Faculty of Electrical Engineering, Mathematics, and Computer Science*, pp. 73–75, 2005.
- [21] B. Cauchi, I. Kodrasi, R. Rehr, S. Gerlach, A. Jukić, T. Gerkmann, S. Doclo, and S. Goetze, "Combination of mvdr beamforming and single-channel spectral processing for enhancing noisy and reverberant speech," *EURASIP Journal on Advances in Signal Processing*, vol. 2015, no. 1, p. 61, 2015. [Online]. Available: <http://dx.doi.org/10.1186/s13634-015-0242-x>
- [22] G. Welch and G. Bishop, "An introduction to the kalman filter," 1995.